# Multiquark states. II. $Q\bar{Q}$ and $Q^2\bar{Q}^2$ mesons

A. T. Aerts,* P. J. Mulders, and J. J. de Swart
*Institute for Theoretical Physics, University of Nijmegen, The Netherlands*
(Received 29 October 1979)

In the previous paper we proposed a phenomenological mass formula based on the MIT bag model. We used it to describe the spectrum of baryon resonances. Now it is applied to the $Q\bar{Q}$ and $Q^2\bar{Q}^2$ states. Using the results for the $Q\bar{Q}$ meson spectrum we are able to perform a parameter-free calculation of the $Q^2$-$\bar{Q}^2$ baryonium spectrum. The other orbitally excited $Q^2\bar{Q}^2$ configurations are also studied. We find natural interpretations for the narrow $N\bar{N}$ resonances, e.g., for the $S(1936)$, which we predict to have $J^{PC}=2^{--}$ and $I=0$, 1, and 2 components.

## I. INTRODUCTION

This paper, which is devoted to the study of the $Q\bar{Q}$ and $Q^2\bar{Q}^2$ systems, is part of a series in which we discuss the masses and some of the decay properties of multiquark systems. In the first paper[1] we explained the structure of the mass spectrum for orbitally and radially excited baryon resonances. There we assumed a quark-diquark (or more generally a two-cluster) structure in a bag,[2] which for orbital excitations is stretched and for large values of the orbital angular momentum $l$ gives rise to linear trajectories.[3] A general formula was given for the mass of a bag containing a definite number of quarks which, except for possible phenomenological (quark-exchange) terms for small $l$ ($l=1$ or 2), becomes

$$M=M_{nl}+M_m. \tag{1}$$

The mass formula contains a multiplet mass $M_{nl}$ and a fine-structure term $M_m$ due to the color-magnetic interaction. We will not consider radial excitations in this paper so we will omit the radial quantum number $n$ and use the notation $M_l$ instead of $M_{nl}$. For the multiplet mass a linear trajectory in the $l$-$M^2$ plane has been assumed,

$$M^2=M_0^2+l/\alpha', \tag{2}$$

where $\alpha'$ is the color-dependent Regge slope. For $l=0$, $M$ reduces to the MIT-bag-model expression[2] for hadrons containing only quarks in the ${}^1s_{1/2}$ ground state of the spherical bag. We will examine the consequences of Eq. (1) for $Q\bar{Q}$ and $Q^2\bar{Q}^2$ orbital excitations.[4]

The $Q\bar{Q}$ orbital excitations have a very simple structure. Each cluster contains only one particle. The fine-structure term $M_m$ is entirely due to the interaction between the quark and the antiquark (two different clusters) and is seen to vanish for large $l$ (Ref. 1). As expected, the $\rho$ and the $\pi$ trajectories become degenerate in the $l$-$M^2$ plane for large $l$. Already for $l=1$ they are very close. The $Q\bar{Q}$ $l=1$ states containing nonstrange quarks all lie around 1250 MeV. For almost all of these states candidates exist in this region (Table V). The scalar mesons $\epsilon(700)$, $S^*(980)$, and $\delta(980)$ do not belong to the ${}^3P_0$ $Q\bar{Q}$ multiplet. They have a very natural interpretation as $l=0$ $Q^2\bar{Q}^2$ states.[5,6] Mass contributions arising from $\vec{I}\cdot\vec{s}$, tensor, and other interactions are small, and can be neglected to first order. We then are able to calculate the masses of the orbitally excited $Q^2\bar{Q}^2$ mesons, which consist of a diquark ($Q^2$) and an antidiquark ($\bar{Q}^2$) cluster, without having to introduce *any free parameters*.

Our way of calculating is rather similar to the one used by Jaffe.[7] However, he includes $M_m$ in the intercept

$$M^2=(M_0+M_m)^2+l/\alpha',$$

and thus gets parallel trajectories in the $l$-$M^2$ plane and an effective color-magnetic splitting which decreases with $l$. We treat the fine structure as an $l$-independent perturbation which in the baryon sector leads to two slightly diverging trajectories in the $l$-$M^2$ plane and gives a better description of the data.

Another similar approach has been proposed by Chan *et al.*[8,9] Their mass formula has the same structure as Eq. (1). The important difference lies in the treatment of the intercept mass and the strength of the fine structure. We estimate these quantities following Ref. 1, using the MIT bag model. Chan *et al.* treat them as free parameters. The fine structure is fixed using the light hadrons. The intercept of each trajectory is fixed by assigning one of the states on it to an experimental candidate. The $Q^2\bar{Q}^2$ system allows color-triplet, -sextet, and -octet trajectories for each of which Chan *et al.* then get a different intercept. The relation between the intercept mass $M_0$ and the physical $l=0$ states is lost this way. In our case Eq. (1) reproduces the masses of the $l=0$ $Q^2\bar{Q}^2$ mesons, and thus our extrapolation to higher $l$ values re-

 

ceives additional support from the successful classification of the lower scalar-meson nonet as $l=0$ $Q^2\bar{Q}^2$ states.

We differ with both authors in our treatment of the color-magnetic splitting strength. Where they effectively take the $l=0$ strength for all values of $l$, the strength we use is a function of the number of quarks, which reside in each bag end.

The $Q^2$-$\bar{Q}^2$ states, particularly the ones in which the diquark is in a color-triplet ($c=3$) state, are of special interest because they couple to the colorless ($c=1$) baryon-antibaryon channels. Many experimental indications for states decaying into $B\bar{B}$ or formed in $B\bar{B}$ annihilation experiments, called baryonia, have been reported with widths in a surprisingly large range (~2–200 MeV). Most of these still have to be confirmed from other sources.

A striking outcome of our parameter-free calculation is the fact that without experimental input from the baryonium sector it allows an easy identification of all prominent low-lying states with $c=3$ $Q^2$-$\bar{Q}^2$ levels. For example, the $S(1936)$ meson is assigned to the $J^{PC}=2^{--}$ member of the complex level at 1.94 GeV, which contains degenerate $I=0$, 1, and 2 multiplets. This identification moreover yields a simple explanation[10] for the suppression of the charge exchange to the elastic $\bar{p}p$ cross section at this energy.

We do not find compelling indications for color-sextet $Q^2$-$\bar{Q}^2$ or color-octet $Q\bar{Q}$-$Q\bar{Q}$ levels in the baryonium spectrum. Nonetheless, these states may exist. It may, however, prove more rewarding to look for them in $e^+e^-$ annihilation experiments. We have therefore given a separate list of all $J^{PC}=1^{--}$ levels in the color-triplet and -sextet $Q^2$-$\bar{Q}^2$ and color-octet $Q\bar{Q}$-$Q\bar{Q}$ spectrum. Further negative evidence in these sectors may point to a fast conversion of the nontrivial color charges into triplet or singlet ones.

Parallel to the bag approach to the $Q^2\bar{Q}^2$ spectrum also the string-junction[11] or topological[12] model have been developed, yielding alternative level schemes.

In addition to the multiquark states coupling to $N\bar{N}$, bound states and resonances due to the $N\bar{N}$ interaction should also occur.[13] However, it is difficult to understand the presence of heavier states ($M>1.95$ GeV) or their narrow widths if exclusively $N\bar{N}$ resonances and bound states are considered. In that case, more involved dynamics is needed. Another distinction is the high degeneracy in spin and isospin, which is inherent to multiquark states and which is very unlikely from a nuclear-potential point of view. A full analysis should take both types of states into account.

The paper is organized as follows. In Sec. II we study the spectrum of $Q\bar{Q}$ mesons. In Sec. III we apply our mass formula to the $Q^2\bar{Q}^2$ states. In Sec. IV we make some comments on the (in)stability of the calculated spectrum. Finally, in Sec. V we discuss various aspects of the spectrum more extensively by means of a comparison with the experimental data.

TABLE I. Eigenvalues of the SU(3) quadratic Casimir operator and the inverse trajectory slope as a function of color.

| $c$ | $f_c^2$ | $1/\alpha'(c)$ (GeV$^2$) |
|---|---|---|
| 3 | $\frac{4}{3}$ | 1.20 |
| 6 | $\frac{10}{3}$ | 1.90 |
| 8 | 3 | 1.80 |
| 10 | 6 | 2.55 |
| 15 | $\frac{16}{3}$ | 2.40 |

## II. $Q\bar{Q}$ MESONS

The masses of the $Q\bar{Q}$ system and its orbital excitations are given by

$$M=M_l+M_m=[M_0^2+l/\alpha'(c)]^{1/2}+M_m. \tag{3}$$

The multiplet mass $M_l$ is color dependent through the slope $\alpha'(c)$ of the Regge trajectory. The slope can be calculated in the string approximation of Johnson and Thorn.[3] In terms of the bag parameters, $B=59$ MeV fm$^{-3}$ and $\alpha_s=g^2/4\pi=2.20$, where $g$ is the quark-gluon coupling, one finds

$$4\pi\alpha'(c)=(2\pi\alpha_s B f_c^2)^{-1/2}. \tag{4}$$

The color dependence is contained in $f_c^2$, the eigenvalue of the color-SU(3) quadratic Casimir operator $F_c^2$ in the $c$-dimensional color irreducible representation (irrep) $c$, to which the quarks couple. For a $Q\bar{Q}$ system one only has color-triplet charges. For this and more general situations, $f_c^2$ and $\alpha'(c)$ are listed in Table I. The computed value $1/\alpha'(3)=1.15$ GeV$^2$ agrees quite well with the experimental value 1.1–1.2 GeV$^2$. Until now only mesons with $l\leq 4$ have been found. They lie on a trajectory with a slope (1.2 GeV$^2$) which seems to be slightly higher than that for baryon trajectories

TABLE II. The color-magnetic interaction strengths (in MeV) $M_{ij}$ between nonstrange ($n$) and/or strange ($s$) quarks as a function of the number of quarks ($N$) in a cluster.

| $N$ | 2 | 3 | 4 |
|---|---|---|---|
| $M_{nn}$ | 85 | 74 | 67 |
| $M_{ns}$ | 70 | 61 | 56 |
| $M_{ss}$ | 58 | 51 | 46 |

TABLE III. $M_l$: the multiplet mass for the $Q\bar{Q}$ system as a function of $l$. The values are calculated from Eqs. (1) and (2) using $1/\alpha'(3) = 1.20$ GeV$^2$.

| $l$ | $I=1$ $(n\bar{n})$ | $I=0$ $(n\bar{n})$ | $I=0$ $(s\bar{s})$ | $I=\frac{1}{2}$ $(n\bar{s}/s\bar{n})$ |
|---|---|---|---|---|
| 0 | 670 | 670 | 990 | 840 |
| 1 | 1285 | 1285 | 1475 | 1380 |
| 2 | 1685 | 1685 | 1835 | 1760 |
| 3 | 2010 | 2010 | 2140 | 2075 |
| 4 | 2290 | 2290 | 2405 | 2345 |
| 5 | 2540 | 2540 | 2640 | 2590 |
| 6 | 2765 | 2765 | 2860 | 2810 |
| 7 | 2975 | 2975 | 3060 | 3015 |
| 8 | 3170 | 3170 | 3250 | 3210 |

(1.1 GeV$^2$). As we will be concerned mainly with low-$l$ states, our results will not be very sensitive to the precise value of the slope. We will take $1/\alpha'(3)=1.2$ GeV$^2$.

For $l=0$, the color-magnetic interaction is given by

$$M_m = m[-(F\sigma)_Q \cdot (F\sigma)_{\bar{Q}}] = m\Delta, \tag{5a}$$

where $m=\alpha_s M(m_Q R, m_{\bar{Q}} R)/R$ is known from the MIT bag model (Table II). For $l\neq 0$, the bag will become stretched and $M_m$ is no longer known. We will assume that the strength $m_{12}$ of the color-magnetic interaction between the quark and the antiquark at different bag ends 1 and 2 will vanish for large $l$. We then get

$$M_m(l) = m_{12}(l)[-(F\sigma)_1 \cdot (F\sigma)_2] = m_{12}(l)\Delta_{12}. \tag{5b}$$

We will estimate $m_{12}(l)$ from the meson spectrum. For mesons, $\Delta_{12}=\Delta=2s(s+1)-3$ splits the triplet ($s=1$) states from the singlet ($s=0$) states.

We have listed both $M_l$ (Table III) and the masses of the experimental[14,15] meson states (Table IV), containing $u$, $d$, and $s$ quarks, except those states we think to have a $Q^2\bar{Q}^2$ configuration, i.e., the lowest $J^{PC}=0^{++}$ mesons and the $N\bar{N}$ resonances listed in Tables XIX and XX. Apart from the $A_1(1100)$, which seems to be a case of its own, and the $\rho'(1600)$, which may be a radial excitation, the assignment of the mesons in Table IV shows a clear clustering of these states in multiplets.

Only for $l=1$ and 2 are we able to estimate the strength of the underlying color-magnetic splitting, since only for these values of $l$ are both singlet and triplet states present. We estimate $m_{12}(l)=\delta_l m_{12}(0)=\delta_l m$ with $\delta_1\simeq 0.2$ and $\delta_2\simeq 0.05$. This is a crude estimate based on the experimental masses of mesons, containing only nonstrange quarks, in which we used the singlet and an (equal weight) average of the triplet mass values. By lack of data we choose $\delta_l=0$ for $l\geq 3$. This is consistent with our treatment of the baryon spectrum. Orbitally excited baryons have a quark-diquark structure. Also in this case the color-magnetic interaction between quarks at different ends does not vanish for $l=1$ and 2, but can be put equal to zero for $l\geq 3$.

Residual interactions are present which lift the degeneracy in total spin $J$ and isospin $I$, e.g., spin-orbit and tensorlike interactions and mixing with other $Q\bar{Q}$ and $Q^2\bar{Q}^2$ states. The resulting mass pattern shows no systematic dominance of any of these interactions. Moreover, their combined effect on the mass values in our assignment

TABLE IV. $Q\bar{Q}$ meson states (experimental). The particles are denoted as a function of their quantum numbers $l$, $J$, $P$, $C$, and $I$. The particle names are separated from their mass (in MeV) by a semicolon. The mass is followed by its error, when known, and by a question mark, when some of its quantum numbers are uncertain. When preceded by a tilde, the mass and possibly also some quantum numbers are not (well) established.

| $l$ | $J^{PC}$ | $I=1$ $(n\bar{n})$ | $I=0$ $(n\bar{n})$ | $I=0$ $(s\bar{s})$ | $I=\frac{1}{2}$ $(n\bar{s}/s\bar{n})$ |
|---|---|---|---|---|---|
| 0 | $0^{-+}$ | $\pi$; 138 | $\eta$; 549 | $\eta'$; 958 | $K$; 496 |
| | $1^{--}$ | $\rho$; 776 ± 3 | $\omega$; 783 | $\phi$; 1020 | $K^*$; 892 |
| 1 | $1^{+-}$ | $B$; 1231 ± 10 | | | $Q_1$; ~1280 |
| | $0^{++}$ | $\delta'$; ~1270 | $\epsilon'$; ~1300 | $\epsilon'$; ~1540 | $\kappa$; ~1400 |
| | $1^{++}$ | $A_1$; ~1100 | $D$; 1276 ± 3 | $E$; 1431 ± 3 | $Q_2$; ~1380 |
| | $2^{++}$ | $A_2$; 1312 ± 5 | $f$; 1271 ± 5 | $f'$; 1516 ± 10 | $K^*$; 1434 ± 5 |
| 2 | $2^{-+}$ | $A_3$; ~1640 | | | $L$; 1765 ± 10 ? |
| | $1^{--}$ | $\rho'$; ~1600 | | | |
| | $2^{--}$ | | | | |
| | $3^{--}$ | $g$; 1688 ± 20 | $\omega$; 1668 ± 10 | | $K^*$; 1784 ± 10 |
| 3 | $3^{+-}$ | | | | |
| | $2^{++}$ | ~1950 | | | |
| | $3^{++}$ | | | | |
| | $4^{++}$ | ~1980 | $h$; 2040 ± 20 | | |

is relatively small. This observation justifies our approximation, in which we only consider the color-magnetic fine structure.

All states listed in Table IV [with the possible exception of $A_1(1100)$ and $\rho'(1600]$ lie on the leading trajectories and their masses are reproduced rather well by our mass formula. We therefore expect that this formula will also describe the mass spectrum of states lying on the leading $Q^2\bar{Q}^2$ trajectories reasonably well.

## III. $Q^2\bar{Q}^2$ ORBITAL EXCITATIONS

Compared to the $Q\bar{Q}$ and $Q^3$ system, the $Q^2\bar{Q}^2$ one is more complicated and offers more possibilities because of its larger number of constituents. A $Q^2\bar{Q}^2$ color singlet can be split into two clusters with definite color in more than one way. It is the smallest multiquark system in which subsystems with nontrivial color charges can appear. Apart from the familiar single-quark ($Q$) cluster, which in the case of $Q^2\bar{Q}^2$ mesons occurs with the color-antitriplet $Q\bar{Q}^2$ one, two-particle clusters can be formed which generate, in addition to the triplet charges, sextet and octet charges (Table V). These larger color charges give rise to trajectories with a slope which differs from the "universal," color-triplet one (Table I). We will refer to the corresponding trajectories as color-sextet ($c=6$) and color-octet ($c=8$) trajectories.

We will start our discussion of the mass spectrum of the $Q^2\bar{Q}^2$ orbital excitations with the most simple system, the $Q^2$-$\bar{Q}^2$ one, which contains a diquark ($Q^2$) and an antidiquark ($\bar{Q}^2$) cluster, separated by an angular momentum barrier (-). We subsequently proceed to the more complicated $Q\bar{Q}$-$Q\bar{Q}$, $Q$-$Q\bar{Q}^2$, and $Q^2\bar{Q}$-$\bar{Q}$ systems.

### A. The $Q^2$-$\bar{Q}^2$ orbital excitations

The masses of these so-called baryonium states are expected to be also given by Eq. (3). No exchange of quarks between the bag ends, such as is encountered in the baryonic $Q^2$-$Q$ configurations, is possible. Furthermore, as we will argue in Sec. IV B, the probability of transition of the $Q^2$-$\bar{Q}^2$ systems to the corresponding $Q$-$Q\bar{Q}^2$ and $Q^2\bar{Q}$-$\bar{Q}$ ones, will generally be rather small. Such transitions, in general, will cause mixing between these two configurations. In this case they will only affect the wave functions a little, but hardly change the mass values.

The multiplet masses are calculated just as for the $Q\bar{Q}$ mesons by using Eq. (2). The intercepts ($M_0$) have been listed in Table VI as a function of the number of strange quarks ($n_s$).

The color-magnetic interaction differs in the $Q\bar{Q}$ and $Q^2\bar{Q}^2$ mesons in one important way. In the $Q^2\bar{Q}^2$ system the interactions between particles in the same cluster are expected to persist for large $l$. This phenomenon is also observed in the spectrum of baryonic orbital excitations. The color-magnetic interaction of the (nonstrange) quarks in the diquark splits the $I=0$ diquark level from that with $I=1$. The combination of a diquark with a nonstrange quark then yields two baryon trajectories, one with $I=\frac{1}{2}$ and another one with both $I=\frac{1}{2}$ and $\frac{3}{2}$. This two-trajectory structure is in excellent agreement with the experimental baryon data. Combination of a diquark with an antidiquark ($Q^2$-$\bar{Q}^2$) gives three baryonium trajectories, for both $c=3$ and $c=6$. One finds one trajectory with $I=0$, two degenerate ones with $I=1$, and one with $I=0$, 1, and 2 (for $n_s=0$).

The fine structure can thus be divided into three parts. There is the color-magnetic interaction between the two quarks which are in one bag end (1), that between the two antiquarks in the other bag end (2), and that between quarks and antiquarks, i.e., between different bag ends (12),

$$M_n=m_1\Delta_1+m_2\Delta_2+m_{12}\Delta_{12}. \tag{6}$$

Using the results of Sec. II we parametrize the interaction between the two clusters as

TABLE V. Two-particle cluster, as a function of the quark content $Q^n\bar{Q}^m$, color $c$, flavor-spin $[\mu]$, flavor $\underline{n}$, and spin $s$. Also, the eigenvalues $\Delta$ of the operator $O=-(F\sigma)_A\cdot(F\sigma)_B$ are given; $A$ and $B$ denote different particles.

| Content | $c$ | $[\mu]$ | $\underline{n}$ | $s$ | $\Delta$ | Name |
|---|---|---|---|---|---|---|
| $Q^2$ | 3* | [21] | $\underline{3}^*$ | 0 | $-2$ | $\chi_1$ |
| | | | $\underline{6}$ | 1 | $\frac{2}{3}$ | $\chi_2$ |
| | 6 | [15] | $\underline{3}^*$ | 1 | $-\frac{1}{3}$ | $\chi_3$ |
| | | | $\underline{6}$ | 0 | 1 | $\chi_4$ |
| $Q\bar{Q}$ | 8 | $[35]\otimes[1]$ | $\underline{9}$ | 1 | $-\frac{1}{6}$ | $\chi_5$ |
| | | | | 0 | $\frac{1}{2}$ | $\chi_6$ |

TABLE VI. Intercepts $M_0$ (in GeV) of the linearized $Q^2\bar{Q}^2$ trajectories as a function of the number of strange quarks $n_s$.

| $n_s$ | $M_0(n_s)$ |
|---|---|
| 0 | 1.458 |
| 1 | 1.634 |
| 2 | 1.802 |
| 3 | 1.965 |
| 4 | 2.121 |

$$m_{12}(l)\Delta_{12}=\delta_l m_{12}(0)\Delta_{12}$$
$$=\delta_l \sum_{i,j=1}^{2}\left(\frac{\alpha_s}{R}\right)M(m_{Q_i}R, m_{\bar{Q}_j}R)[-(F\sigma)_i\cdot(F\sigma)_j]$$
$$=\delta_l\left[\left(\frac{\alpha_s}{R}\right)\sum_{i,j=1}^{2}M(m_{Q_i}R, m_{\bar{Q}_j}R)\right]$$
$$\times[-(F\sigma)_Q\cdot(F\sigma)_{\bar{Q}}], \tag{7}$$

in terms of the spherical bag functions (Table II), evaluated at the radius of the $l=0$ $Q^2\bar{Q}^2$ bag. The color-spin part can be taken out of the summation because the two (anti)quarks reside in the same cluster and are indistinguishable. Using the results of Ref. 1 the interaction between the quarks in the same bag end is given by

$$m_1\Delta_1=\frac{\alpha_s}{R_1}M(m_Q R_1, m_Q, R_1)[-(F\sigma)_Q\cdot(F\sigma)_{Q'}], \tag{8}$$

again in terms of the spherical bag functions, but now evaluated at a radius $R_1=r_0 N_1^{1/3}$, where $r_0=3.63$ GeV$^{-1}$ and $N_1$ is the number of quarks in bag end 1; in this case $N_1=2$. One finds an expression similar to Eq. (8) for the antiquarks. Proceeding in this way, we avoid the introduction of new parameters.

We will now evaluate the color and spin part of the color-magnetic interaction. This is most conveniently done when we construct the baryonium states from diquark and antidiquark basis states. The diquark clusters are taken to have definite color (so $M_l$ is diagonal in this basis) and spin. We assumed that the two particles in the diquark both have the same spatial wave function, associated with the lowest energy. This implies, because of Fermi-Dirac statistics, that the diquark also has definite flavor. With respect to this basis the two-quark operator

$$\Delta_1=-(F\sigma)_Q\cdot(F\sigma)_{Q'}$$
$$=(\tfrac{4}{3}-\tfrac{1}{2}F_{QQ'}{}^2)(2S_{QQ'}{}^2-3) \tag{9}$$

is diagonal (Table V). $S_{QQ'}{}^2=\frac{1}{4}(\sigma_Q+\sigma_{Q'})^2$ and $F_{QQ'}{}^2=(F_Q+F_{Q'})^2$ are the quadratic Casimir operators for spin and color, respectively. A similar result holds for the antidiquark. For such simple systems it is thus sufficient to know the color SU(3, $c$) and the spin SU(2, $s$) content of the states. The quantum numbers of the resulting spectrum are given in Table VII.

Using the fact that the diquark belongs to the flavor-spin SU(6, fs) irrep $[\mu]=[21]$ for $c=3$ and

TABLE VII. Properties of the color-singlet two-quark-cluster product states [notation $(i,j)\equiv\chi_i\otimes\chi_j$; for $\chi_i$ see Table V]. One has $P=(-1)^l$ under space inversion, where $l$ is the orbital angular momentum, which can be even ($e$) or odd ($o$). One can form linear combinations of the neutral hyperchange $Y=0$ members of the degenerate flavor multiplets $\underline{18}$ and $\underline{18}^*$ of either charge parity $C_n=\eta=\pm$. For the $G$ parity one has $G=(-1)^I C_n$, where $I$ is the isospin of the $Y=0$ flavor-multiplet member. $\Delta$ gives the size of the color-magnetic splitting.

| Trajectory | Product state | $s$ | $\underline{n}$ | $C_n$ | $l$ | $\Delta$ |
|---|---|---|---|---|---|---|
| $c=3$ | (1,1) | 0 | $\underline{9}$ | $(-1)^l$ | $e$ and $o$ | $-4$ |
| | (1,2) | 1 | $\underline{18}^*$ | $\pm$ | $e$ and $o$ | $-\frac{4}{3}$ |
| | (2,1) | 1 | $\underline{18}$ | | | |
| | (2,2) | 0,1,2 | $\underline{36}$ | $(-1)^{l+s}$ | $e$ and $o$ | $\frac{4}{3}$ |
| $c=6$ | (3,3) | 0,1,2 | $\underline{9}$ | $(-1)^{l+s}$ | $e$ and $o$ | $-\frac{2}{3}$ |
| | (3,4) | 1 | $\underline{18}^*$ | $\pm$ | $e$ and $o$ | $\frac{2}{3}$ |
| | (4,3) | 1 | $\underline{18}$ | | | |
| | (4,4) | 0 | $\underline{36}$ | $(-1)^l$ | $e$ and $o$ | 2 |
| $c=8$ | (5,5) | 0,2 | $\underline{9}\oplus\underline{36}$ | + | $e$ | $-\frac{1}{3}$ |
| | | 1 | $\underline{18}\oplus\underline{18}^*$ | $\pm$ | $e$ | |
| | | 0,2 | $\underline{18}\oplus\underline{18}^*$ | $\pm$ | $o$ | |
| | | 1 | $\underline{9}\oplus\underline{36}$ | + | $o$ | |
| | (5,6) | 1 | $\underline{9}\oplus\underline{36}$ | $(-1)^{l+1}$ | $e$ and $o$ | $\frac{1}{3}$ |
| | (6,5) | | $\underline{18}\oplus\underline{18}^*$ | $\pm$ | $e$ and $o$ | |
| | (6,6) | 0 | $\underline{9}\oplus\underline{36}$ | + | $e$ | 1 |
| | | | $\underline{18}\oplus\underline{18}^*$ | $\pm$ | $o$ | |

TABLE VIII. Recoupling matrices for SU(2): $(J_{Q^2}, J_{\bar{Q}^2}; J) \leftrightarrow (J_{Q\bar{Q}}, J_{Q'\bar{Q}'}; J)$: $\eta = +$; $(J_{Q\bar{Q}'}, J_{Q'\bar{Q}}; J) \leftrightarrow (J_{Q\bar{Q}}, J_{Q'\bar{Q}'}; J)$: $\eta = -$.

| | $J=0$ | | $J=2$ |
|---|---|---|---|
| | (1,1;0) | (0,0;0) | (1,1;2) |
| (1,1;0) | $-\frac{1}{2}$ | $\frac{1}{2}(\eta\sqrt{3})$ | (1) |
| (0,0;0) | $\frac{1}{2}(\eta\sqrt{3})$ | $\frac{1}{2}$ | |

| | $J=1$ | | |
|---|---|---|---|
| | (1,1;1) | (1,0;1) | (0,1;1) |
| (1,1;1) | 0 | $\frac{\eta}{\sqrt{2}}$ | $\frac{1}{\sqrt{2}}$ |
| (1,0;1) | $\frac{\eta}{\sqrt{2}}$ | $\frac{1}{2}$ | $-\frac{\eta}{2}$ |
| (0,1;1) | $\frac{1}{\sqrt{2}}$ | $-\frac{\eta}{2}$ | $\frac{1}{2}$ |

$[\mu]=[15]$ for $c=6$, we find that, independent of $l$, the $c=3$ trajectory states will be $[21]\otimes[21^*]$ states, and those on the $c=6$ trajectory $[15]\otimes[15^*]$ ones.

Also when $\delta_l \neq 0$ the antiquark-quark interactions contribute to the mass. We therefore need to know the content of each $(QQ')$ $(\bar{Q}\bar{Q}')$ state in terms of its $(Q\bar{Q})$ $(Q'\bar{Q}')$ subsystems, since $\Delta_{12}$ is diagonal in that basis. This requires the recoupling matrices for both spin and color (Tables VIII and IX). Because of the symmetry of the $Q^2$-$\bar{Q}^2$ states it does not matter which of the quarks and antiquarks are combined in a particular $Q\bar{Q}$ system. The result is that for $l=1$ and 2 the $Q\bar{Q}$ interaction causes a small amount of mixing between those states on the $c=3$ and $c=6$ trajectories that have the same angular momentum $l$, and total spin $s$.

The resulting mass spectrum is listed in Tables X and XI. Equation (6) predicts for a multiplet with definite values $c$, $n_s$, and $l>2$ (so $m_{12}=0$) an equal spacing of levels ($\Delta M$). When the difference between two successive multiplet masses has about the same size as $\Delta M$ we get accidental degeneracy between levels with different $l$. For $c=3$ and $n_s=0$ we find a clustering of levels near $M=2.25$, 2.51, and 2.72 GeV. It is encouraging to know that this clustering is also observed experimentally, be it at somewhat lower masses, i.e., ~2.18, ~2.35, and ~2.50 GeV. This gives an indication of the effects not included when one computes the mass of broad ($\Gamma \gtrsim 200$ MeV) states in a zero-width approximation.

### B. The $Q\bar{Q}$-$Q\bar{Q}$ orbital excitations

There are two important differences between the $Q\bar{Q}$-$Q\bar{Q}$ and the $Q^2$-$\bar{Q}^2$ orbital excitations. The first is that the former behaves as a two-boson system rather than two two-fermion systems. Secondly, the distribution of the (anti)quarks over the two clusters gives rise to exchange contributions to the mass for small values of $l$.

A $Q\bar{Q}$ system can occur in a color-singlet and a color-octet state. Only the latter generates the color-electric field necessary to confine two such

TABLE IX. Recoupling matrices for SU(3): $(\underline{n}_{Q^2}, \underline{n}_{\bar{Q}^2}; \underline{n}) \leftrightarrow (\underline{n}_{Q\bar{Q}}, \underline{n}_{Q'\bar{Q}'}; \underline{n})$; $(\underline{n}_{Q\bar{Q}'}, \underline{n}_{Q'\bar{Q}}; \underline{n}') \leftrightarrow (\underline{n}_{Q\bar{Q}}, \underline{n}_{Q'\bar{Q}'}; \underline{n}')$.

| | $\underline{n}=\underline{1}$ | |
|---|---|---|
| | $(1,1;\underline{1})$ | $(8,8;\underline{1})$ |
| $(\underline{3}^*,\underline{3};\underline{1})$ | $-\left(\frac{1}{3}\right)^{1/2}$ | $-\left(\frac{2}{3}\right)^{1/2}$ |
| $(\underline{6},\underline{6}^*;\underline{1})$ | $\left(\frac{2}{3}\right)^{1/2}$ | $-\left(\frac{1}{3}\right)^{1/2}$ |

| | $\underline{n}'=\underline{1}$ | |
|---|---|---|
| | $(\underline{1},\underline{1};\underline{1})$ | $(\underline{8},\underline{8};\underline{1})$ |
| $(1,1;\underline{1})$ | $\frac{1}{3}$ | $-\frac{2\sqrt{2}}{3}$ |
| $(8,8;\underline{1})$ | $-\frac{2\sqrt{2}}{3}$ | $-\frac{1}{3}$ |

| | $\underline{n}=\underline{8}$ | | | |
|---|---|---|---|---|
| | $(\underline{8},\underline{8};\underline{8}_d)$ | $(\underline{8},\underline{8};\underline{8}_f)$ | $(\underline{1},\underline{8};\underline{8})$ | $(\underline{8},\underline{1};\underline{8})$ |
| $(\underline{3}^*,\underline{3};\underline{8})$ | $\left(\frac{5}{6}\right)^{1/2}$ | 0 | $-\frac{1}{\sqrt{12}}$ | $-\frac{1}{\sqrt{12}}$ |
| $(\underline{6},\underline{6}^*;\underline{8})$ | $\frac{1}{\sqrt{6}}$ | 0 | $\left(\frac{5}{12}\right)^{1/2}$ | $\left(\frac{5}{12}\right)^{1/2}$ |
| $(\underline{3}^*,\underline{3}^*;\underline{8})$ | 0 | $\frac{1}{\sqrt{2}}$ | $\frac{1}{2}$ | $-\frac{1}{2}$ |
| $(6,3;\underline{8})$ | 0 | $\frac{1}{\sqrt{2}}$ | $-\frac{1}{2}$ | $\frac{1}{2}$ |

| $\underline{n}=\underline{10}$ | $\underline{n}=\underline{10}^*$ | $\underline{n}=\underline{27}$ |
|---|---|---|
| $(\underline{8},\underline{8};\underline{10})$ | $(\underline{8},\underline{8};\underline{10}^*)$ | $(\underline{8},\underline{8},\underline{27})$ |
| $(\underline{6},\underline{3};\underline{10})$ (1) | | $(\underline{6},\underline{6}^*;\underline{27})$ (1) |

clusters in one orbitally excited bag. The $Q\bar{Q}$-$Q\bar{Q}$ states then are most easily classified using a two-(colored) meson basis. Consequently, the allowed quantum numbers of these states are found by imposing Bose-Einstein statistics and therefore depend on $l$ being odd or even (Table VII). The total range of flavor-spin quantum numbers for the two mesons is contained in the direct product $[36]\otimes[36]$, which is also contained in the diquark $\otimes$ antidiquark product representations $\{[15]\oplus[21]\}$ $\otimes\{[15^*]\oplus[21^*]\}$. For even $l$ only the representations $[15]\otimes[15^*]$ and $[21]\otimes[21^*]$ occur in the $Q\bar{Q}$-$Q\bar{Q}$ spectrum which are also available in the $Q^2$-$\bar{Q}^2$ spectrum. For odd $l$ only those contained in $[15]$ $\otimes[21^*]$ and $[21]\otimes[15^*]$ can occur. These flavor-spin configurations are forbidden in the $Q^2$-$\bar{Q}^2$ system.

For $l=1$ and 2 the spatial wave functions of the quarks still overlap. This overlap results in a direct ($\Delta M_l$) and an exchange ($M_e$) contribution which we can parametrize for the baryon excitations,[1] but not in this case because of the total absence of prominent experimental candidates. For the baryons $\Delta M_l$ and $M_e$ are of the order of 100 MeV for $l=1$ and considerably smaller for $l=2$. Since we expect that the overlap will have a similar effect on the "mesonium"[16] states, $M_e$ and $\Delta M_l$ probably also will give a positive mass contribution here. The magnitude of these two terms is hard to estimate, since the mesonium configuration differs from the baryonic one and e.g., does not contain tunneling contributions (Sec. IV B). We therefore

TABLE X. Masses and quantum numbers $(\underline{f},l,s,J,P,C_n,n_s)$ of the color $c=3$ baryonia. One has $G=C_n\,(-1)^I$.

| | $JC_n$ | $\underline{f}$ | $s$ | $n_s/0$ | 1 | 2 | | 3 | 4 |
|---|---|---|---|---|---|---|---|---|---|
| | | | | | | $s=2$ | $s=0$ | | |
| $l^P=1^-$ | $1-$ | $\underline{9}$ | 0 | 1.50 | 1.66 | | 1.83 | | |
| | $0\pm\ 1\pm\ 2\pm$ | $\underline{18}\oplus\underline{18}^*$ | 1 | 1.72 | 1.85–1.87 | 1.98 | 2.02 | 2.15 | |
| | $1-$ | $\underline{36}$ | 0 | 1.86 | 2.00 | 2.14 | 2.14 | 2.28 | 2.42 |
| | $0+\ 1+\ 2+$ | $\underline{36}$ | 1 | 1.90 | 2.04 | 2.17 | 2.17 | 2.31 | 2.44 |
| | $1-\ 2-\ 3-$ | $\underline{36}$ | 2 | 1.94 | 2.07 | 2.21 | 2.21 | 2.34 | 2.47 |
| $l^P=2^+$ | $2+$ | | | 1.76 | 1.92 | | 2.07 | | |
| | $1\pm\ 2\pm\ 3\pm$ | | | 2.01 | 2.13–2.17 | 2.24 | 2.28 | 2.40 | |
| | $2+$ | | | 2.23 | 2.34 | 2.46 | 2.46 | 2.58 | 2.70 |
| | $1-\ 2-\ 3-$ | | | 2.23 | 2.35 | 2.47 | 2.47 | 2.58 | 2.70 |
| | $0+\ 1+\ 2+\ 3+\ 4+$ | | | 2.24 | 2.36 | 2.48 | 2.48 | 2.59 | 2.71 |
| $l^P=3^-$ | $3-$ | | | 2.05 | 2.17 | | 2.31 | | |
| | $2\pm\ 3\pm\ 4\pm$ | | | 2.28 | 2.38–2.42 | 2.48 | 2.52 | 2.63 | |
| | $3-$<br>$2+\ 3+\ 4+$<br>$1-\ 2-\ 3-\ 4-\ 5-$ | | | 2.50 | 2.61 | 2.71 | 2.71 | 2.82 | 2.92 |
| $l^P=4^+$ | $4+$ | | | 2.29 | 2.39 | | 2.53 | | |
| | $3\pm\ 4\pm\ 5\pm$ | | | 2.52 | 2.61–2.65 | 2.70 | 2.74 | 2.84 | |
| | $4+$<br>$3-\ 4-\ 5-$<br>$2+\ 3+\ 4+\ 5+\ 6+$ | | | 2.75 | 2.84 | 2.93 | 2.93 | 3.03 | 3.13 |
| $l^P=5^-$ | $5-$ | | | 2.51 | 2.60 | | 2.73 | | |
| | $4\pm\ 5\pm\ 6\pm$ | | | 2.74 | 2.82–2.86 | 2.91 | 2.95 | 3.04 | |
| | $5-$<br>$4+\ 5+\ 6+$<br>$3-\ 4-\ 5-\ 6-\ 7-$ | | | 2.96 | 3.05 | 3.14 | 3.14 | 3.23 | 3.32 |
| $l^P=6^+$ | $6+$ | | | 2.71 | 2.80 | | 2.92 | | |
| | $5\pm\ 6\pm\ 7\pm$ | | | 2.94 | 3.02–3.06 | 3.10 | 3.14 | 3.22 | |
| | $6+$<br>$5-\ 6-\ 7-$<br>$4+\ 5+\ 6+\ 7+\ 8+$ | | | 3.17 | 3.25 | 3.33 | 3.33 | 3.41 | 3.50 |
| $l^P=7^-$ | $7-$ | | | 2.90 | 2.99 | | 3.11 | | |
| | $6\pm\ 7\pm\ 8\pm$ | | | 3.13 | 3.21–3.25 | 3.29 | 3.33 | 3.41 | |
| | $7-$<br>$6+\ 7+\ 8+$<br>$5-\ 6-\ 7-\ 8-\ 9-$ | | | 3.36 | 3.44 | 3.52 | 3.52 | 3.60 | 3.69 |

cannot include these terms in the mass, which then is given by Eqs. (3) and (6).

The color-magnetic interaction strengths $m_1$ and $m_2$ and the values of $\Delta_1$ and $\Delta_2$ [Eq. (6)] can be found in Tables II and V, respectively. In order to calculate $\Delta_{12}$, one has to know the recoupling of the $Q\bar{Q}$-$Q'\bar{Q}'$ wave functions to the $QQ'$-$\bar{Q}\bar{Q}'$ and the $Q\bar{Q}'$-$Q'\bar{Q}$ ones (Tables VIII and IX). The strength $m_{12}$ of this term can be parametrized as before.

The masses of the mesonium states obtained from Eq. (3) are listed in Table XII. We expect that the values, quoted for $l=1$ (and 2), may be somewhat low since we did not include $M_e$ and $\Delta M_I$.

We finally note that the terms $m_{12}\Delta_{12}$, $\Delta M_I$, and $M_e$ are not diagonal in the two-meson basis. This implies that they will mix states containing two color-octet mesons with those containing two color-singlet ones. Therefore, mesonium states are unstable in a way similar to the $l=0$ $Q^2\bar{Q}^2$ states.

### C. The $Q$-$Q\bar{Q}^2$ and $Q^2\bar{Q}$-$\bar{Q}$ orbital excitations

The single-quark cluster has to be combined with a color-antitriplet $Q\bar{Q}^2$ cluster in order to form a color-singlet $Q^2\bar{Q}^2$ system. Analyzing the $(Q\bar{Q})\,\bar{Q}$ content of this color-triplet $Q\bar{Q}^2$ cluster we find that the $(Q\bar{Q})$ subsystem can be both a color octet and a color singlet. Therefore, these orbital excitations are similar to the $l=0$ $Q^2\bar{Q}^2$ states[5] and most of them are probably nonresonant[6] since they lie above the lowest threshold of the $MM^*$ channels they couple to. $M$ is an $l=0$ $Q\bar{Q}$ meson; $M^*$ has $l\neq 0$.

Up to exchange contributions the mass of these $c=3$ trajectory states can be computed using Eqs. (3) and (6). The fine structure for this system ($n_s=0$) is given by

$$M_m = m_1\Delta_1 + m_{12}\Delta_{12}. \tag{10}$$

The strength of the color-magnetic splitting inside the three-quark cluster in terms of the mass $m$ of

TABLE XI. Masses and quantum numbers $(f, l, s, J, P, C_n, n_s)$ of the color $c=6$ baryonia. One has $C_n=(-1)^I$.

| | $JC_n$ | $f$ | $s$ | $n_s/0$ | 1 | 2 ($s=2$) | 2 ($s=0$) | 3 | 4 |
|---|---|---|---|---|---|---|---|---|---|
| $l^P=1^-$ | $1-$ | $\underline{9}$ | 0 | 1.87 | 2.01 | | 2.15 | | |
| | $0+\ 1+\ 2+$ | | 1 | 1.91 | | | 2.18 | | |
| | $1-\ 2-\ 3-$ | | 2 | 2.01 | 2.14 | | 2.27 | | |
| | $0\pm\ 1\pm\ 2\pm$ | $\underline{18}\oplus\underline{18}^*$ | 1 | 2.06 | 2.18–2.20 | 2.31 | 2.31 | 2.43 | |
| | $1-$ | $\underline{36}$ | 0 | 2.17 | 2.29 | 2.41 | 2.40 | 2.52 | 2.64 |
| $l^P=2^+$ | $2+$ | | | 2.35 | 2.47 | | 2.58 | | |
| | $1-\ 2-\ 3-$ | | | 2.36 | | | 2.59 | | |
| | $0+\ 1+\ 2+\ 3+\ 4+$ | | | 2.39 | 2.51 | | 2.62 | | |
| | $1\pm\ 2\pm\ 3\pm$ | | | 2.49 | 2.59–2.61 | 2.70 | 2.70 | 2.80 | |
| | $2+$ | | | 2.60 | 2.70 | 2.81 | 2.79 | 2.90 | 3.00 |
| $l^P=3^-$ | $3-$ | | | 2.75 | 2.84 | | 2.95 | | |
| | $2+\ 3+\ 4+$ | | | | | | | | |
| | $1-\ 2-\ 3-\ 4-\ 5-$ | | | | | | | | |
| | $2\pm\ 3\pm\ 4\pm$ | | | 2.84 | 2.94–2.96 | 3.03 | 3.03 | 3.13 | |
| | $3-$ | | | 2.93 | 3.05 | 3.15 | 3.11 | 3.22 | 3.31 |
| $l^P=4^+$ | $4+$ | | | 3.06 | 3.16 | | 3.25 | | |
| | $3-\ 4-\ 5-$ | | | | | | | | |
| | $2+\ 3+\ 4+\ 5+\ 6+$ | | | | | | | | |
| | $3\pm\ 4\pm\ 5\pm$ | | | 3.17 | 3.25–3.27 | 3.34 | 3.34 | 3.42 | |
| | $4+$ | | | 3.28 | 3.36 | 3.45 | 3.43 | 3.51 | 3.59 |
| $l^P=5^-$ | $5-$ | | | 3.35 | 3.44 | | 3.52 | | |
| | $4+\ 5+\ 6+$ | | | | | | | | |
| | $3-\ 4-\ 5-\ 6-\ 7-$ | | | | | | | | |
| | $4\pm\ 5\pm\ 6\pm$ | | | 3.47 | 3.53 – 3.55 | 3.62 | 3.62 | 3.69 | |
| | $5-$ | | | 3.57 | 3.64 | 3.72 | 3.71 | 3.78 | 3.86 |
| $l^P=6^+$ | $6+$ | | | 3.62 | 3.70 | | 3.78 | | |
| | $5-\ 6-\ 7-$ | | | | | | | | |
| | $4+\ 5+\ 6+\ 7+\ 8+$ | | | | | | | | |
| | $5\pm\ 6\pm\ 7\pm$ | | | 3.73 | 3.80–3.82 | 3.87 | 3.87 | 3.95 | |
| | $6+$ | | | 3.84 | 3.90 | 3.98 | 3.96 | 4.04 | 4.10 |

TABLE XII. Masses and quantum numbers $(\underline{f}, l, s, J, P, C_n, n_s)$ of the color $c=8$ mesonia. One has $C_n=(-1)^I$.

| | $JC_n$ | $\underline{f}$ | $s$ | $n_s/0$ | 1 | 2 $s=2$ | 2 $s=0$ | 3 | 4 |
|---|---|---|---|---|---|---|---|---|---|
| $l^P=1^-$ | $1\pm$ | $\underline{18}\oplus\underline{18}^*$ | 0 | 1.94 | 2.07 | 2.20 | 2.16 | 2.31 | |
| | $0+\ 1+\ 2+$ | $\underline{9}\oplus\underline{36}$ | 1 | 1.96 | 2.09 | 2.21 | 2.18 | 2.33 | 2.45 |
| | $0\pm\ 1\pm\ 2\pm$ | $\underline{18}\oplus\underline{18}^*$ | 1 | 1.98 | 2.12 | 2.25 | 2.27 | 2.40 | |
| | $1\pm\ 2\pm\ 3\pm$ | $\underline{18}\oplus\underline{18}^*$ | 2 | 1.99 | 2.11 | 2.25 | 2.25 | 2.38 | |
| | $0+\ 1+\ 2+$ | $\underline{9}\oplus\underline{36}$ | 1 | 2.00 | 2.12 | 2.24 | 2.24 | 2.38 | 2.55 |
| | $1\pm$ | $\underline{18}\oplus\underline{18}^*$ | 0 | 2.01 | 2.13 | 2.26 | 2.29 | 2.42 | |
| $l^P=2^+$ | $2+$ | $\underline{9}\oplus\underline{36}$ | 0 | 2.38 | 2.48 | 2.59 | 2.58 | 2.70 | 2.80 |
| | $1\pm\ 2\pm\ 3\pm$ | $\underline{18}\oplus\underline{18}^*$ | 1 | 2.38 | 2.49 | 2.60 | 2.58 | 2.70 | |
| | $0+\ 1+\ 2+\ 3+\ 4+$ | $\underline{9}\oplus\underline{36}$ | 2 | 2.39 | 2.49 | 2.61 | 2.60 | 2.72 | 2.83 |
| | $1-\ 2-\ 3-$ | $\underline{9}\oplus\underline{36}$ | 1 | 2.40 | 2.50 | 2.62 | 2.61 | 2.73 | 2.87 |
| | $1\pm\ 2\pm\ 3\pm$ | $\underline{18}\oplus\underline{18}^*$ | 1 | 2.40 | 2.50 | 2.62 | 2.64 | 2.76 | |
| | $2+$ | $\underline{9}\oplus\underline{36}$ | 0 | 2.42 | 2.52 | 2.63 | 2.66 | 2.77 | 2.91 |
| $l^P=3^-$ | $3\pm$ | $\underline{18}\oplus\underline{18}^*$ | 0 | 2.72 | 2.81 | 2.91 | 2.91 | 3.02 | |
| | $1\pm\ 2\pm\ 3\pm\ 4\pm\ 5\pm$ | $\underline{18}\oplus\underline{18}^*$ | 2 | | | | | | |
| | $2+\ 3+\ 4+$ | $\underline{9}\oplus\underline{36}$ | 1 | | | | | | 3.13 |
| | $2+\ 3+\ 4+$ | $\underline{9}\oplus\underline{36}$ | 1 | 2.77 | 2.85 | 2.96 | 2.95 | 3.05 | 3.16 |
| | $2\pm\ 3\pm\ 4\pm$ | $\underline{18}\oplus\underline{18}^*$ | 1 | | 2.87 | | 2.97 | 3.06 | |
| | $3\pm$ | $\underline{18}\oplus\underline{18}^*$ | 0 | 2.83 | 2.91 | 3.00 | 3.00 | 3.10 | |
| $l^P=4^+$ | $4+$ | $\underline{9}\oplus\underline{36}$ | 0 | 3.03 | 3.11 | 3.20 | 3.20 | 3.30 | 3.40 |
| | $3\pm\ 4\pm\ 5\pm$ | $\underline{18}\oplus\underline{18}^*$ | 1 | | | | | | |
| | $2+\ 3+\ 4+\ 5+\ 6+$ | $\underline{9}\oplus\underline{36}$ | 2 | | | | | | 3.40 |
| | $3-\ 4-\ 5-$ | $\underline{9}\oplus\underline{36}$ | 1 | 3.08 | 3.16 | 3.25 | 3.24 | 3.34 | 3.44 |
| | $3\pm\ 4\pm\ 5\pm$ | $\underline{18}\oplus\underline{18}^*$ | 1 | | 3.17 | | 3.26 | 3.35 | |
| | $4+$ | $\underline{9}\oplus\underline{36}$ | 0 | 3.14 | 3.21 | 3.29 | 3.29 | 3.38 | 3.47 |
| $l^P=5^-$ | $5\pm$ | $\underline{18}\oplus\underline{18}^*$ | 0 | 3.31 | 3.39 | 3.47 | 3.47 | 3.56 | |
| | $3\pm\ 4\pm\ 5\pm\ 6\pm\ 7\pm$ | $\underline{18}\oplus\underline{18}^*$ | 2 | | | | | | |
| | $4+\ 5+\ 6+$ | $\underline{9}\oplus\underline{36}$ | 1 | | | | | | 3.66 |
| | $4+\ 5+\ 6+$ | $\underline{9}\oplus\underline{36}$ | 1 | 3.36 | 3.43 | 3.52 | 3.51 | 3.60 | 3.69 |
| | $4\pm\ 5\pm\ 6\pm$ | $\underline{18}\oplus\underline{18}^*$ | 1 | | 3.44 | | 3.53 | 3.61 | |
| | $5\pm$ | $\underline{18}\oplus\underline{18}^*$ | 0 | 3.42 | 3.49 | 3.56 | 3.56 | 3.64 | |
| $l^P=6^+$ | $6+$ | $\underline{9}\oplus\underline{36}$ | 0 | 3.57 | 3.64 | 3.72 | 3.72 | 3.80 | 3.89 |
| | $5\pm\ 6\pm\ 7\pm$ | $\underline{18}\oplus\underline{18}^*$ | 1 | | | | | | |
| | $4+\ 5+\ 6+\ 7+\ 8+$ | $\underline{9}\oplus\underline{36}$ | 2 | | | | | | 3.89 |
| | $5-\ 6-\ 7-$ | $\underline{9}\oplus\underline{36}$ | 1 | 3.62 | 3.68 | 3.76 | 3.75 | 3.84 | 3.93 |
| | $5\pm\ 6\pm\ 7\pm$ | $\underline{18}\oplus\underline{18}^*$ | 1 | | 3.70 | | 3.78 | 3.85 | |
| | $6+$ | $\underline{9}\oplus\underline{36}$ | 0 | 3.68 | 3.74 | 3.81 | 3.81 | 3.88 | 3.96 |

a nonstrange quark is given by

$$m_1=(\alpha_s/R)M(mR,mR) \tag{11}$$

with $R=r_0(3)^{1/3}$. In Tables XIII–XVI we have listed the recoupling matrices for color and spin, the composition of the basic cluster states, and the occurring two-particle operators $O=-(F\sigma)_1\cdot(F\sigma)_2$ for the $Q^2\bar{Q}$-$\bar{Q}$ configuration. The color-magnetic interaction of the two quarks in the $Q^2\bar{Q}$ system is identical to the corresponding interaction in the

TABLE XIII. Recoupling matrices for SU(3): $(\underline{n_{Q^2}}, \underline{n_{\bar{Q}}}; \underline{n_{Q^2\bar{Q}}}) \longleftrightarrow (\underline{n_{Q\bar{Q}}}, \underline{n_Q}; \underline{n_{Q^2\bar{Q}}})$.

| | $(\underline{8},\underline{3};\underline{3})$ | $(\underline{1},\underline{3};\underline{3})$ |
|---|---|---|
| $(\underline{6},\ \underline{3}^*;\underline{3})$ | $-(\frac{1}{3})^{1/2}$ | $(\frac{2}{3})^{1/2}$ |
| $(\underline{3}^*,\underline{3}^*;\underline{3})$ | $(\frac{2}{3})^{1/2}$ | $(\frac{1}{3})^{1/2}$ |

TABLE XIV. Recoupling matrices for SU(2): $(j_{Q^2}, j_{\bar{Q}}; j_{Q^2\bar{Q}}) \longleftrightarrow (j_{Q\bar{Q}}, j_Q; j_{Q^2\bar{Q}})$.

| | $(1,\frac{1}{2};\frac{1}{2})$ | $(0,\frac{1}{2};\frac{1}{2})$ |
|---|---|---|
| $(1,\frac{1}{2};\frac{1}{2})$ | $-\frac{1}{2}$ | $(\frac{3}{4})^{1/2}$ |
| $(0,\frac{1}{2};\frac{1}{2})$ | $(\frac{3}{4})^{1/2}$ | $\frac{1}{2}$ |

TABLE XV. Quantum numbers of the color-singlet three ⊗ one-quark-cluster product states.

| $C_{Q^2}$ | $j_{Q^2}$ | $j_{Q^2\bar{Q}}$ | $j_{Q^2\bar{Q}^2}$ | $\underline{n}_{Q^2}$ | $\underline{n}_{Q^2\bar{Q}}$ | $\underline{n}_{Q^2\bar{Q}^2}$ | Name |
|---|---|---|---|---|---|---|---|
| 3* | 0 | $\frac{1}{2}$ | 0,1 | | | | $\phi_1$ |
| 6 | 1 | $\frac{1}{2}$ | 0,1 | $\underline{3}^*$ | $\underline{3}\oplus\underline{6}^*$ | $\underline{9}\oplus\underline{18}^*$ | $\phi_2$ |
| | | $\frac{3}{2}$ | 1,2 | | | | $\phi_3$ |
| 6 | 0 | $\frac{1}{2}$ | 0,1 | | | | $\phi_4$ |
| 3* | 1 | $\frac{1}{2}$ | 0,1 | $\underline{6}$ | $\underline{3}\oplus\underline{15}$ | $\underline{18}\oplus\underline{36}$ | $\phi_5$ |
| | | $\frac{3}{2}$ | 1,2 | | | | $\phi_6$ |

$Q^2\bar{Q}^2$ system. Also, the interaction of the antiquark with one of the quarks in the $Q^2\bar{Q}$ cluster has its counterpart in those $Q^2\bar{Q}^2$ states in which both antiquarks have the same interactions with the diquark. Since in a $Q^2\bar{Q}$ cluster the number of interactions is only half that in the $Q^2\bar{Q}^2$ one, we find that $\Delta_1$ is precisely a half times $\Delta$ for the corresponding $Q^2\bar{Q}^2$ state. Using Tables XIII–XVI, $\Delta_{12}$ can also be constructed.[4] For states also containing strange quarks it is convenient and sufficiently accurate to replace $m_1$ in Eq. (11) by

$$m_1(n_s)=\frac{\alpha_s}{3R}\left[M(m_Q R, m_{Q'}R)+M(m_Q R, m_{\bar{Q}}R)+M(m_{Q'}R, m_{\bar{Q}}R)\right] \quad (12)$$

and $m_{12}$ by a similar expression. The masses computed with this prescription are listed in Table XVII.

The flavor-spin content of the $Q^2\bar{Q}$-$\bar{Q}$ spectrum is quite different from that of the $l=0$ $Q^2\bar{Q}^2$ one because the antiquarks in the former multiquark configuration are distinguishable. Combination of the $Q^2\bar{Q}$ flavor-spin representations, contained in $\{[21]\otimes[15]\}\otimes[6^*]$ with the $[6^*]$ of the second antiquark, yields $\{[21]\oplus[15]\}\otimes\{[21^*]\oplus[15^*]\}$ for the $Q^2\bar{Q}$-$\bar{Q}$ representations. To obtain the physical states one has to take those linear combinations of the $Q^2\bar{Q}$-$\bar{Q}$ and the conjugate (degenerate) $Q$-$Q\bar{Q}^2$ states, which diagonalize $G$ parity, when they have zero hypercharge. Every flavor-spin multiplet then occurs with both $C_n=+$ and $-$. The number of available states will then be about four times as large as for the $Q^2$-$\bar{Q}^2$ configuration.

Also in the $Q^2\bar{Q}$-$\bar{Q}$ system antiquark exchange is possible. We expect that e.g., the $l=1$ $Q^2\bar{Q}$-$\bar{Q}$ states in which the color-spin-flavor part of the $(\bar{Q}\bar{Q})$ wave function is antisymmetric will be somewhat heavier than the symmetric combinations.

Although the existence of the $Q\bar{Q}$ color-singlet subsystem does not favor stability, we note that as large a splitting as associated with $\Delta_1=-5.42$ may (for small $l$ values) already push this level below the relevant $MM^*$ thresholds.

## IV. STABILITY

There are several mechanisms through which an orbitally excited $Q^2\bar{Q}^2$ state can decay into two- or more-particle final states. We will discuss the ones we think are most relevant to the stability of the above calculated spectrum.

### A. Fission

The only systems that may fission into two-particle final states are those containing three-quark clusters. From the color recoupling matrix in Table XIII we see that the $Q\bar{Q}$ in the $c=3$ cluster is for at least 30% a color singlet which, in principle, is no longer confined to the cluster. One thinks here of reaction chains like $(Q^2\bar{Q})_3$-$(\bar{Q})_{3*}$ $\to[(Q\bar{Q})_1(Q)_3]_3$-$(\bar{Q})_{3*}\to(Q\bar{Q})_1(Q_3$-$\bar{Q}_{3*})\to$ mesons. Here the subscripts denote the color.

The angular momentum can be distributed over the final state in several ways. The emitted meson $(Q\bar{Q})$ is most naturally in its ground state $(\pi,\rho)$. It may be excited, but for small $l$ this is quite unfavorable. The remaining fragment $(Q$-$\bar{Q})$ will usually have angular momentum $l'\leq l$. Possible differences between $l'$ and $l$ depend on the an-

TABLE XVI. Matrix representations of the two-particle operators. The eigenvectors and eigenvalues $\Delta$ of the matrix $\Delta_1=2A+B$, $A=-(F\partial)_Q\cdot(F\partial)_{\bar{Q}}$, and $B=-(F\partial)_Q\cdot(F\partial)_{Q'}$.

| $A$ | $B$ | Basis | Eigenvector | | $\Delta$ |
|---|---|---|---|---|---|
| $\begin{bmatrix} 0 & -(\frac{2}{3})^{1/2} \\ -(\frac{2}{3})^{1/2} & -\frac{5}{3} \end{bmatrix}$ | $\begin{bmatrix} -2 & 0 \\ 0 & -\frac{1}{3} \end{bmatrix}$ | $\phi_1$ | $\begin{bmatrix} 0.582 \\ 0.813 \end{bmatrix}$ | $\begin{bmatrix} 0.813 \\ -0.582 \end{bmatrix}$ | −5.42 |
| | | $\phi_2$ | | | −0.25 |
| $\frac{1}{3}$ | $\frac{2}{3}$ | $\phi_3$ | 1 | | $\frac{4}{3}$ |
| $\begin{bmatrix} 0 & -(\frac{2}{3})^{1/2} \\ -(\frac{2}{3})^{1/2} & -\frac{2}{3} \end{bmatrix}$ | $\begin{bmatrix} 1 & 0 \\ 0 & \frac{2}{3} \end{bmatrix}$ | $\phi_4$ | $\begin{bmatrix} 0.813 \\ 0.582 \end{bmatrix}$ | $\begin{bmatrix} -0.582 \\ 0.813 \end{bmatrix}$ | −2.42 |
| | | $\phi_5$ | | | 2.75 |
| $\frac{5}{6}$ | $-\frac{1}{3}$ | $\phi_6$ | 1 | | $\frac{4}{3}$ |

TABLE XVII. Masses and quantum numbers $[f, l, s, J, P=(-)^l, C_n=\pm, n_s]$ of the color-3 $Q^2\bar{Q}$-$\bar{Q}$ and $Q$-$Q\bar{Q}^2$ states. $n^3-n$ etc., gives the distribution of the (non)strange quarks over the clusters. The superscript on $J$ gives the multiplicity.

| $J$ | $f$ | $n^3-n$ | $n^3-s$ | $n^2s-n$ | $n^2s-s$ | $ns^2-n$ | $ns^2-s$ | $s^3-n$ | $s^3-s$ |
|---|---|---|---|---|---|---|---|---|---|
| $l^P=1^-$ | | | | | | | | | |
| $0, 1^2, 2$ | $\underline{9}\oplus\underline{18}^*$ | 1.34 | 1.49 | 1.55 | 1.69 | 1.73 | 1.87 | | |
| $0, 1^2, 2$ | $\underline{18}\oplus\underline{36}$ | 1.61 | 1.75 | 1.78 | 1.92 | 1.94 | 2.08 | 2.10 | 2.24 |
| $0, 1^2, 2$ | $\underline{9}\oplus\underline{18}^*$ | 1.80 | 1.94 | 1.95 | 2.09 | 2.09 | 2.23 | | |
| $0, 1^2, 2^2, 3$ | $\underline{9}\oplus\underline{18}^*$ | 1.94 | 2.09 | 2.07 | 2.21 | 2.20 | 2.34 | | |
| $0, 1^2, 2^2, 3$ | $\underline{18}\oplus\underline{36}$ | 1.94 | 2.09 | 2.07 | 2.21 | 2.20 | 2.34 | 2.33 | 2.47 |
| $0, 1^2, 2$ | $\underline{18}\oplus\underline{36}$ | 2.07 | 2.21 | 2.18 | 2.32 | 2.30 | 2.44 | 2.42 | 2.56 |
| $l^P=2^+$ | | | | | | | | | |
| $1, 2^2, 3$ | | 1.71 | 1.83 | 1.88 | 2.01 | 2.05 | 2.17 | | |
| $1, 2^2, 3$ | | 1.94 | 2.06 | 2.09 | 2.21 | 2.23 | 2.36 | 2.37 | 2.50 |
| $1, 2^2, 3$ | | 2.11 | 2.23 | 2.24 | 2.36 | 2.36 | 2.49 | | |
| $0, 1^2, 2^2, 3^2, 4$ | | 2.23 | 2.36 | 2.34 | 2.47 | 2.46 | 2.58 | | |
| $0, 1^2, 2^2, 3^2, 4$ | | 2.23 | 2.36 | 2.34 | 2.47 | 2.46 | 2.58 | 2.57 | 2.70 |
| $1, 2^2, 3$ | | 2.34 | 2.47 | 2.44 | 2.56 | 2.54 | 2.67 | 2.65 | 2.77 |
| $l^P=3^-$ | | | | | | | | | |
| $2, 3^2, 4$ | | 1.99 | 2.10 | 2.15 | 2.27 | 2.30 | 2.42 | | |
| $2, 3^2, 4$ | | 2.21 | 2.33 | 2.35 | 2.46 | 2.48 | 2.59 | 2.61 | 2.72 |
| $2, 3^2, 4$ | | 2.37 | 2.49 | 2.49 | 2.60 | 2.60 | 2.72 | | |
| $1, 2^2, 3^2, 4^2, 5$ | | 2.49 | 2.60 | 2.59 | 2.70 | 2.69 | 2.81 | | |
| $1, 2^2, 3^2, 4^2, 5$ | | 2.49 | 2.60 | 2.59 | 2.70 | 2.69 | 2.81 | 2.80 | 2.91 |
| $2, 3^2, 4$ | | 2.60 | 2.71 | 2.68 | 2.80 | 2.78 | 2.89 | 2.87 | 2.99 |
| $l^P=4^+$ | | | | | | | | | |
| $3, 4^2, 5$ | | 2.23 | 2.33 | 2.38 | 2.49 | 2.52 | 2.63 | | |
| $3, 4^2, 5$ | | 2.45 | 2.55 | 2.58 | 2.68 | 2.70 | 2.80 | 2.82 | 2.93 |
| $3, 4^2, 5$ | | 2.61 | 2.71 | 2.72 | 2.82 | 2.82 | 2.93 | | |
| $2, 3^2, 4^2, 5^2, 6$ | | 2.73 | 2.83 | 2.82 | 2.92 | 2.91 | 3.02 | | |
| $2, 3^2, 4^2, 5^2, 6$ | | 2.73 | 2.83 | 2.82 | 2.92 | 2.91 | 3.02 | 3.01 | 3.12 |
| $3, 4^2, 5$ | | 2.84 | 2.94 | 2.91 | 3.02 | 3.00 | 3.10 | 3.08 | 3.19 |
| $l^P=5^-$ | | | | | | | | | |
| $4, 5^2, 6$ | | 2.45 | 2.54 | 2.59 | 2.69 | 2.73 | 2.83 | | |
| $4, 5^2, 6$ | | 2.67 | 2.77 | 2.79 | 2.88 | 2.90 | 3.00 | 3.02 | 3.12 |
| $4, 5^2, 6$ | | 2.83 | 2.93 | 2.93 | 3.03 | 3.03 | 3.13 | | |
| $3, 4^2, 5^2, 6^2, 7$ | | 2.95 | 3.04 | 3.03 | 3.13 | 3.12 | 3.22 | | |
| $3, 4^2, 5^2, 6^2, 7$ | | 2.95 | 3.04 | 3.03 | 3.13 | 3.12 | 3.22 | 3.21 | 3.31 |
| $4, 5^2, 6$ | | 3.06 | 3.15 | 3.12 | 3.22 | 3.20 | 3.30 | 3.28 | 3.38 |
| $l^P=6^+$ | | | | | | | | | |
| $5, 6^2, 7$ | | 2.65 | 2.74 | 2.79 | 2.88 | 2.92 | 3.01 | | |
| $5, 6^2, 7$ | | 2.88 | 2.96 | 2.99 | 3.08 | 3.09 | 3.19 | 3.20 | 3.30 |
| $5, 6^2, 7$ | | 3.04 | 3.12 | 3.13 | 3.22 | 3.22 | 3.31 | | |
| $4, 5^2, 6^2, 7^2, 8$ | | 3.15 | 3.24 | 3.23 | 3.32 | 3.31 | 3.40 | | |
| $4, 5^2, 6^2, 7^2, 8$ | | 3.15 | 3.24 | 3.23 | 3.32 | 3.31 | 3.40 | 3.39 | 3.49 |
| $5, 6^2, 7$ | | 3.26 | 3.35 | 3.32 | 3.41 | 3.39 | 3.49 | 3.47 | 3.56 |

gular momentum between the $Q\bar{Q}$ and $Q$-$\bar{Q}$ systems. Of course $l < l'$ may occur, but is less probable in view of phase space and couplings.

Examining the simplest case, the emission of an unexcited $Q\bar{Q}$ meson in an $s$ wave, we find from Tables XIII–XVI that for states with $j_{Q^2\bar{Q}}=\frac{1}{2}$, the meson is a pseudoscalar ($P$) or a vector meson ($V$); for states with $j_{Q^2\bar{Q}}=\frac{3}{2}$ it must be a vector meson. It may always be an isovector particle ($\pi$, $\rho$). Against such a decay mode the states with $\Delta = -5.42$ and $\Delta=\frac{4}{3}$ seem to be most stable, coupling to $P^*P$ and $P^*V$, respectively. For $l=1$ these states presumably are less than 100 MeV above threshold. Since $P^*$ and $V^*$, in this case the $l=1$ $P$ and $V$ excitations, are not very narrow sharp signals at the relevant two-body thresholds, such as e.g., the $\delta(980)$ and $S^*(980)$ in the case of $l=0$ $Q^2\bar{Q}^2$ systems, may not be expected. The final state will then contain three or more mesons.

For higher $l$ the $Q^2\bar{Q}$-$\bar{Q}$ states will lie much

closer to, and often even below, the $MM^*(l'=l)$ threshold. This is due to the fact that the difference between $M_l$ for $Q\bar{Q}$ and $Q^2\bar{Q}^2$ states and that between $M_l$ and $M_{l+1}$ decreases with increasing $l$, whereas the color-magnetic splitting remains constant. The emission of $M$ in a $P$ or higher $L$ wave will allow decay to $MM^*(l'<l)$ final states. This decay mode is more favorable energetically but this advantage is obtained at the cost of a larger angular momentum barrier. Below threshold the higher $L$ values are necessary for decay and may reduce the partial width for this mode. For these $l$ values also decay into two excited mesons among other decay modes will become a more favored decay mode, with a larger partial width.

Already for $l=1$ states emission of $M$ in a $P$ wave may dominate the $S$-wave decay mode. Both mesons are now in their ground state.

### B. Tunneling

In Ref. 1 we studied the mass spectrum of the $Q^3$ baryon orbital excitations consisting of a diquark and a quark cluster. We demonstrated that for $l=1$ and 2 the spatial wave function of quarks in the two clusters overlap. This leads to tunneling and exchange mass contributions. In the $Q^2$-$Q$ system the mass term due to tunneling of one of the quarks is proportional to the term due to the exchange of the other two quarks. We expect this overlap to also be present for the $Q^2\bar{Q}^2$ states with $l=1$ and 2. For a system like $Q^2$-$\bar{Q}^2$, the effect of this overlap on the mass will only be of second order. It does not give an exchange term. One needs two tunneling transitions to get a contribution to the mass, e.g., $Q^2$-$\bar{Q}^2 \to Q$-$Q\bar{Q}^2 \to Q^2$-$\bar{Q}^2$. This contribution will be an order of magnitude smaller than for the $Q^2$-$Q$ baryons and presumably negligible. The effect on the wave function, viz., through $Q$-$Q\bar{Q}^2$ and $Q^2\bar{Q}$-$\bar{Q}$ admixtures, is larger and will especially be noticeable in the changes it causes in the decay pattern.

The $Q$-$Q\bar{Q}^2$ and $Q\bar{Q}$-$Q\bar{Q}$ masses will contain exchange contributions for $l=1$. These may be of the same order of magnitude as in the corresponding baryonic case. Note that there are exchange contributions in cases in which tunneling is not possible, because of the absence of intermediate states with proper quantum numbers. Tunneling of a quark in a $Q$-$Q\bar{Q}^2$ state can couple this state to a two-color-singlet-meson final state with angular momentum $l$. For $l=1$ it is identical to the $P$-wave emission discussed in Sec. IV A.

Also gluons ($c=8$) may tunnel from one bag end to the other. They may change the color of a cluster, but then they must also change its spin because of Fermi-Dirac statistics (for $Q^2$-$\bar{Q}^2$) or $G$ parity (for $Q\bar{Q}$). This mode then is only another way of looking at the color-magnetic interaction and this is already accounted for. As already stated, it causes mixing between the $c=6$ and $c=3$ trajectories and between $c=8$ trajectory and $c=1$ free meson states and impairs the stability of the $c=8$ states. This mixing may allow production of some $c=6$ baryonium states[8] near zero momentum transfer ($t=0$) in case of $Q^2\bar{Q}^2$ exchange.

### C. Pair creation

The major decay mode for all those $Q^2\bar{Q}^2$ excitations which cannot fission directly into two color-singlet systems, i.e., mainly those containing two-particle clusters, is the creation of a $Q\bar{Q}$ pair followed by fission into two or more hadrons.

The simplest possibility is the creation from the vacuum. The color-singlet $Q\bar{Q}$ pair then has $J^{PC}I^G = 0^{++}0^+$, corresponding to a $^3P_0$ configuration [quark-pair-creation (QPC) or $^3P_0$ model]. One assumes that the original quarks do not change their spin, color, and flavor state during the creation process, but recombine with the new quarks to form final-state hadrons.

Besides being a rather adequate approach to the strong decays of mesons,[17] it also accounts pretty well for the decay of baryonic ($Q^2$-$Q$) resonances to meson-baryon final states.[1,18] Using the QPC model one can try to select the $c=3$ baryonium states, which are most prominent in the $N\bar{N}$ channels.[7] We will use it to estimate branching ratios.[4] The model can of course also be used to describe the formation of resonances by considering the annihilation of a $Q\bar{Q}$ pair in the initial state.[10]

The addition of a $c=3$ $Q$ or $\bar{Q}$ to a cluster can reduce its color charge. Also, the orbital angular momentum $L$ in the final state can be lower than that in the initial one since the $Q\bar{Q}$ pair is created in a $P$ wave, so $L=|l\pm1|$. In terms of quark clusters one finds the following recombination possibilities:

(a) $(Q^2)_{3^*}+Q \to (Q^3)_c$, $c=1$ or 8 ($B_1$ or $B_8$).
(b) $(Q^2)_{3^*}+\bar{Q} \to (Q^2\bar{Q})_c$, $c=3$ or $6^*$.
(c) $(Q^2)_6+Q \to (Q^3)_c$, $c=8$ or 10 ($B_8$ or $B_{10}$).
(d) $(Q^2)_6+\bar{Q} \to (Q^2\bar{Q})_c$, $c=3$ or 15.
(e) $(Q\bar{Q})_8+Q \to (Q^2\bar{Q})_c$, $c=3$, $6^*$, or 15.

The influence of the color of the cluster on the decay mode can be shown by a simple computation. Applying the mass formula [Eq. (3)] to the $Q^3\bar{Q}^3$ system, we find an intercept mass ($n_s=0$) $M_0 = 2.125$ GeV (Ref. 4). The color-magnetic interaction has for $N=3$ a strength $M_{nn}=75$ MeV (Table II). A classification of $Q^3$ clusters and the masses of the $L=1$ to 3 $Q^3\bar{Q}^3$ excitations have been given in Table XVIII. Comparison of Tables XVIII with Tables X and XI indicates that even in case of strong color-magnetic interactions between the

TABLE XVIII. Quantum numbers of the baryonic $Q^3$ clusters and the persistent part of the orbital $Q^3$-$\bar{Q}^3$ excitation masses or mass intervals for $c=8$ and 10. Masses in GeV.

| $c$ | Flavor-spin | $I$ | $s$ | $\Delta$ | $M_1$ | $M_2$ | $M_3$ |
|---|---|---|---|---|---|---|---|
| 1 | [56] | $\frac{1}{2}$ | $\frac{1}{2}$ | $-2$ | $\geq 1.87$ | $\geq 1.87$ | $\geq 1.87$ |
| | | $\frac{3}{2}$ | $\frac{1}{2}$ | 2 | | | |
| 8 | [70] | $\frac{1}{2}$ | $\frac{1}{2}$ | $-\frac{1}{2}$ | (2.40, 2.85) | (2.70, 3.20) | (3.00, 3.45) |
| | | | $\frac{3}{2}$ | $\frac{1}{2}$ | | | |
| | | $\frac{3}{2}$ | $\frac{1}{2}$ | $\frac{5}{2}$ | | | |
| 10 | [20] | $\frac{1}{2}$ | $\frac{1}{2}$ | 1 | 2.75 | 3.20 | 3.55 |

clusters, the lightest $L=1$ $B_8\bar{B}_8$ excitations lie above the heaviest $l=2$ $c=3$ $Q^2$-$\bar{Q}^2$ states. So only $B_1\bar{B}_1$ occurs in the final state. Similarly, in each of the cases (b) to (d) only the states with the smaller color charge are accessible. The recombination of the $Q\bar{Q}$ cluster with a $Q$ or $\bar{Q}$ may yield, for $l=2$ or 3, color-sextet clusters, but the gain in energy for transitions to the unstable $(Q^2\bar{Q})_3$ cluster is so much larger that it is highly favored.

In the transition of a $(Q^2)_6$ cluster, the unstable $(Q^2\bar{Q})_3$ cluster is favored as a final state over the stable, more heavy $(Q^3)_8$ state. The $c=6$ baryonia will thus decay to multimeson final states. For the $c=3$ $Q^2$-$\bar{Q}^2$ excitations the color is not lowered in case (b) whereas in case (a) color singlets $(B_1\bar{B}_1)$ can be formed in the final state. The latter mode is then presumably dominant in analogy with the previous case, at least above the $B\bar{B}$ threshold. Also in the baryonic case the two-singlet mode, viz., $Q^2$-$Q \to Q^3$-$Q\bar{Q} \to B+M$ in an $L$ wave (yielding, e.g., $N\pi, \Delta\pi, N\rho, \ldots$ final states), seems to be highly preferred to the one in which an excited baryon occurs in the intermediate state, viz., $Q^2$-$Q \to Q^2\bar{Q}$-$Q^2 \to B^*+M \to B+M+M$.

When the $Q\bar{Q}$ pair only recombines with one cluster it will not change its color, but may affect the stability, because it can trigger so-called cascade decays.[19] Explicitly,

$$(Q^2)_{3^*}+(Q'\bar{Q})_1 \to (Q'Q)_c+(Q\bar{Q})_c,$$

$$(c, c')=(3^*, 1),\ (3^*, 8) \text{ or } (6, 8);$$

$$(Q^2)_6+(Q'\bar{Q})_1 \to (Q'Q)_c+(Q\bar{Q})_c,$$

$$(c, c')=(6, 1),\ (3^*, 8) \text{ or } (6, 8);$$

$$(Q\bar{Q})_8+(Q'\bar{Q}')_1 \to (Q\bar{Q}')_c+(Q'\bar{Q})_c,$$

$$(c, c')=(1, 8),\ (8, 1) \text{ or } (8, 8).$$

The excitation decays to a lower one with the same quark and color structure, but usually different flavor and spin structure under emission of a meson (usually a pion). The meson could also take away angular momentum when this proves favorable.

One has, in addition, the possibilities

$$(Q^2)_{3^*}+(Q\bar{Q})_1 \to (Q^3)_c+(\bar{Q})_{3^*} \text{ with } c=1 \text{ or } 8,$$

$$(Q^2)_6+(Q\bar{Q})_1 \to (Q^3)_c+(\bar{Q})_{3^*} \text{ with } c=8 \text{ or } 10.$$

For $c=3$ $Q^2$-$\bar{Q}^2$ states a(n) (anti)baryon (preferably a nucleon) can be emitted and again one may find both $B\bar{B}$ and multimeson final states.

A variant on this decay mode is the creation of a two-gluon pair with $J^{PC}I^G=0^{++}0^+$. In this case color-singlet configurations can be formed when a gluon ($c=8$) combines with a $(Q\bar{Q})_8$ cluster. The rotational energy, released in such a recombination, is larger than in the decay $Q^2$-$\bar{Q}^2 \to B_1\bar{B}_1$ (mode a). This may make the $c=8$ $Q\bar{Q}$-$Q\bar{Q}$ trajectory states very unstable.

## V. ASSIGNMENTS AND DISCUSSION

We will now discuss the experimental candidates for our calculated spectrum. They are listed in Tables XIX and XX. We distinguish between broad (Table XIX) and narrow (Table XX) states, and we will concentrate on the latter, since the predicted masses of these states will agree more precisely with the experimental ones in the zero-width approximation. We assume that the final-state interactions will shift the position of the poles of the narrow states only slightly, whereas their influence on the poles of the broad states may be much greater.

Let us consider the most prominent $N\bar{N}$ resonances at 1.897, 1.936, 2.020, and 2.204 GeV. The lower two states have been seen in $N\bar{N}$ formation experiments, which is a strong indication that they do not contain strange quarks and are color-triplet $Q^2$-$\bar{Q}^2$ states. Also, the $M^0(2020)$, although it has not been seen in a formation experiment, has a large $N\bar{N}$ branching ratio (see below). It therefore is probably also a color-triplet $Q^2$-$\bar{Q}^2$ state. Although for the $M(2204)$ a color-sextet assignment cannot be excluded, a color-triplet

TABLE XIX. Possible candidates for broad baryonium states.

| Mass (GeV) | Width (MeV) | Source (Ref.) | Quantum numbers |
|---|---|---|---|
| 1.95 | 80 | $\bar{p}p \to \rho^0\omega^0, \bar{p}p, \bar{n}n$ (22) | $I^G = 1^-, J^P = 2^+$ or $4^+$ |
| 1.95 | 240 | $\pi^- p \to (\bar{p}p)_F n$ (23) | $J^{PC} = 1^{--}, I^G = 1^+$ |
| 2.01 | 100 | $\bar{p}p \to K^0 K^\pm \pi^\mp$ (24) | |
| 2.15 | 200 | $\bar{p}p \to \pi^+\pi^-, K^+K^-$ (25) | $J^{PC}I^G = 3^{--}, 0^- \& 1^+$ |
| 2.185 | 130 | $\sigma_T, \sigma_{el}$ in $\bar{p}p$ (26) | $I = 1$ |
| 2.31 | 210 | $\bar{p}p \to \pi^+\pi^-, \pi^0\pi^0, K^+K^-$ (25) | $J^{PC}I^G = 4^{++}, 0^+$ |
| 2.35 | 190 | $\sigma_T, \sigma_{el}$ in $\bar{p}p$ (26) | $I = 1$ |
| 2.385 | 80 | $\sigma_T, \sigma_{el}$ in $\bar{p}p$ (26) | $I = 0$ |
| 2.48 | 280 | $\bar{p}p \to \pi^+\pi^-, K^+K^-$ (25) | $J^{PC}I^G = 5^{--}, 0^- \& 1^+$ |

assignment is very plausible since the state has been seen in the same experiment as the $S(1936)$ and the $M(2020)$ and also has a considerable $N\bar{N}$ branching ratio (<16%). Table XXI lists the $Q^2$-$\bar{Q}^2$ states with $n_s = 0$, which couple to $N\bar{N}$ and contain color-triplet diquarks. All our assignments are made taking the calculated masses at face value.

The resonance at 1.897 GeV was found in in-flight annihilation of $\bar{p}d$ going over into charged pions or kaons. It has a complex structure of which an $I = 1$ component seems to have been established through the odd-pion decay mode. The pre-

TABLE XX. Possible candidates for narrow baryonium states.

| Mass (GeV) | Width (MeV) | Source (Ref.) | Quantum numbers |
|---|---|---|---|
| 1.395 | ≤34 | $\gamma$ from atomic $\bar{p}p$ (27) | |
| 1.470 | 10 | $e^+e^-, \bar{p}p$ annihilation (28) | $J^{PC} = 1^{--}$ |
| 1.646 | ≤21 | $\gamma$ from atomic $\bar{p}p$ (27) | |
| 1.684 | ≤19 | $\gamma$ from atomic $\bar{p}p$ (27) | |
| 1.795 | <8 | $\bar{p}d$ annihilation at rest (29) | |
| | | $\not\to 3\pi$, $\not\to 5\pi$ | |
| 1.820 | ~25 | $e^+e^-, \bar{p}p$ annihilation (28) | $J^{PC} = 1^{--}$ |
| 1.875 | <10 | $\bar{p}d$ annihilation at rest (30) | $I^G = 1^+$ |
| 1.897 | 25 | $\bar{p}d$ annihilation in flight (31) | complex; $I = 1$ |
| 1.936 | 3 | $\sigma_T, \sigma_{el}$ in $\bar{p}p$ (32) | complex |
| | | $\sigma_{CEX}$ in $\bar{p}p$ (33) | |
| 1.954 | ≤10 | $\pi^+ p \to \pi^+ p(\bar{p}p)_F$ (34) | |
| 1.975 | <2 | $\bar{n}p \to N$ pions, dip in $\sigma_A$ (35) | $I^G = 1^-$ |
| 1.986 | ~8 | $\bar{n}p \to (K\bar{K}\pi)\pi$ (35) | $I = 1$ |
| 2.020 | 24 ± 12 | $\pi^- p \to p_F(\bar{p}p\pi^-)$ (36) | $I = 0$? |
| | | $e^- p \to e^- p(p\bar{p})$ | |
| 2.110 | 10 | $K^- p \to (\Lambda\bar{p})p$ (37) | |
| 2.130 | 30 | $e^+e^-$ annihilation (28) | $J^{PC} = 1^{--}$ |
| 2.204 | $16^{+20}_{-12}$ | $\pi^+ p \to p_F(\bar{p}p\pi^+)$ (36) | $I = 0$? |
| 2.207 | | $\bar{p}p \to \pi^+_F(\pi^-K^+K^-)$ (38) | $I = 1$ |
| 2.461 | <10 | $K^+ p \to (\bar{\Lambda}p\pi^+)_F n$ (39) | $S = +1, Q = +2$ |
| 2.85 | <40 | $\bar{p}n \to \pi^- X^0$ (40) | $I = 0$? |

TABLE XXI. Selected color-triplet $Q^2$-$\bar{Q}^2$ states, which couple to $N\bar{N}$.

| | $M$ | Representation | $s$ | $I^G$ | $J^{PC}$ | $S$ | $L$ |
|---|---|---|---|---|---|---|---|
| $l^P=1^-$ | 1.90 | (3,3) | 1 | $0^+$ $(1^-)$ | $0^{-+}$ | 0 | 0 |
| | | | | $0^+$ $(1^-)$ | $2^{-+}$ | | 2 |
| | 1.94 | | 2 | $0^-$ $(1^+)$ | $1^{--}$ | 1 | 0 |
| | | | | | | | 2 |
| | | | | $0^-$ $(1^+)$ | $2^{--}$ | 1 | 2 |
| | | | | $0^-$ $(1^+)$ | $3^{--}$ | 1 | 2 |
| $l^P=2^+$ | 2.01 | $[(1,3)+(3,1)]/\sqrt{2}$ | 1 | $1^+$ | $1^{+-}$ | 0 | 1 |
| | | | | | $3^{+-}$ | | 3 |
| | | $[(1,3)-(3,1)]/\sqrt{2}$ | 1 | $1^-$ | $1^{++}$ | 1 | 1 |
| | | | | | $2^{++}$ | | 1 |
| | | | | | | | 3 |
| | | | | | $3^{++}$ | | 3 |
| | 2.23 | (3,3) | 0 | $0^+$ $(1^-)$ | $2^{++}$ | 1 | 1 |
| | | | | | | | 3 |
| | 2.23 | | 1 | $0^-$ $(1^+)$ | $1^{+-}$ | 0 | 1 |
| | | | | $0^-$ $(1^+)$ | $3^{+-}$ | | 3 |
| | 2.24 | | 2 | $0^+$ $(1^-)$ | $0^{++}$ | 1 | 1 |
| | | | | $0^+$ $(1^-)$ | $1^{++}$ | | 1 |
| | | | | $0^+$ $(1^-)$ | $2^{++}$ | | 1 |
| | | | | | | | 3 |
| | | | | $0^+$ $(1^-)$ | $3^{++}$ | | 3 |
| | | | | $0^+$ $(1^-)$ | $4^{++}$ | | 3 |
| $l^P=3^-$ | 2.05 | (1,1) | 0 | $0^-$ | $3^{--}$ | 1 | 2 |
| | | | | | | | 4 |

dicted level at 1.90 GeV has $J^{PC}=0^{-+}$ and $2^{-+}$ components, both with $I=0$ and $I=1$, coupling to the $N\bar{N}$ $^1S_0$ and $^1D_2$ waves, respectively. The $I=1$ state can decay into three or five pions, the $I=0$ state into four, six, or more. In view of the momentum of the incident proton (250 MeV/$c$), the $D$-wave and $J^{PC}=2^{-+}$ assignment may be preferable.

The $S$ resonance at 1.936 GeV has been seen in a number of experiments ($\sigma_T$, $\sigma_{el}$, $\sigma_A$ in $\bar{p}p$). It also has been produced, viz., backwards in $\pi^+p \to (p_F\pi^+)\bar{p}p$. The predicted level at 1.94 GeV contains degenerate $I^G=0^-$, $1^+$, and $2^-$ states each with $J^{PC}=1^{--}$, $2^{--}$, and $3^{--}$. Since the $\pi\pi$ mode is absent in the $S$ decay, we prefer the $J^{PC}=2^{--}$ assignment. It then couples to the $^3D_2$ $N\bar{N}$ wave. A candidate for the $J^{PC}=1^{--}$ level may be the $1^{--}$ state at 1.95 GeV found in a $\pi\pi$ partial-wave analysis. It has a large width, consistent with its coupling to the $^3S_1$ $N\bar{N}$ channel.

The identification of the $S$ with the 1.94-GeV level has another attractive feature. The presence of degenerate $I=0$ and $I=1$ multiplets explains[10] why the charge-exchange process $\bar{p}p \to \bar{n}n$ is not seen, whereas the elastic process $\bar{p}p \to \bar{p}p$ is quite clearly visible. Both $\bar{p}p$ and $\bar{n}n$ are mixtures of isospin eigenstates $[(I, I_z)]$, $\bar{p}p = [(1,0)+(0,0)]/\sqrt{2}$, and $\bar{n}n = [(1,0)-(0,0)]/\sqrt{2}$. The coupling $g$ of the $S$ to the $N\bar{N}$ channels depends on the isospin of these levels. Their ratio, due to isospin recoupling, is $g(I=0):g(I=1)=\sqrt{2}:\sqrt{3}$ (see Sec. IV C, $^3P_0$ model). In the amplitude $A$ for the reaction $N\bar{N} \to S \to N\bar{N}$, the coupling constant $g$ enters twice. Assuming charge independence, one then finds constructive interference in the elastic process whereas the charge-exchange process displays destructive interference. This results in the ratio $\sigma_{el}:\sigma_{CE}=25:1$ for the cross section. Of course, these $Q^2$-$\bar{Q}^2$ states do not exclusively couple to $N\bar{N}$. The meson decay modes will not be the same for the two isospin multiplets ($G$ parity) and therefore the ratio may be somewhat different. In case only one multiplet is present, $\sigma_{el}$ and $\sigma_{CE}$ must be equal, in disagreement with observation. In that case one has to invoke strong interference with the background[20] to obtain the desired suppression. Also, in an $N\bar{N}$ potential model,[21] degenerate $I=0$ and 1 levels can be generated in the $J=L$ channels. One then has to assume dominance of isoscalar $t$-channel exchange. In this model the $S(1936)$ is identified with the $J^{PC}=2^{-+}$, $I=0$ and 1 levels.

Perhaps the most striking examples of baryonium states are the narrow neutral states at 2.020 and 2.204 GeV, quite far above the $N\bar{N}$ threshold. They were first detected[36] in the process $\pi^+p \to B_F^{++}M^0$, which requires baryon exchange (Fig. 1). The forward $B_F^{++}$ is a $\Delta^{++}(1232)$ decaying into $p\pi^+$ and $M^0$ decays into $\bar{p}p$. One has searched for

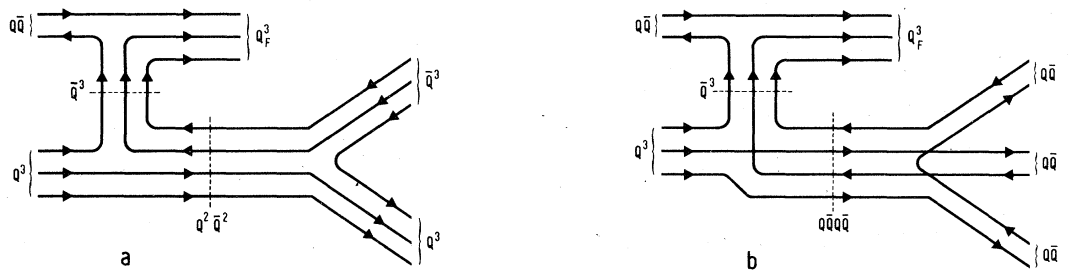


FIG. 1. Harari-Rosner diagrams for the production of a 3-baryonium (a) or 8-mesonium (b) state. The production of a 6-baryonium state proceeds as in diagram (a), only this time a multimeson final state is more probable.

charged partners ($M^-$) in related processes, but until now they have not been found. The state at 2.02 GeV has also been produced by a virtual photon in the reaction $\gamma_v p \to p(\bar{p}p)$ (Ref. 15), but has not been seen in formation experiments. At 2.207 GeV a narrow state has been observed in the process $\bar{p}p \to \pi_F^+(K^+K^-\pi^-)$, suggesting an isovector character.

There are four possible assignments for the $M(2020)$. One could consider the color-triplet levels at 2.01 GeV ($I=1$, $J^{PC}=1^{+\pm}$, $2^{++}$, and $3^{+\pm}$) and 2.05 GeV ($I=0$, $J^{PC}=1^{--}$, $2^{--}$, and $3^{--}$) and the color-sextet levels at 2.01 GeV ($I=0$, $J^{PC}=1^{--}$, $2^{--}$, and $3^{--}$) and at 206 GeV ($I=0$, $J^{PC}=0^{-+}$, $1^{--}$, and $2^{-+}$). We prefer the color-triplet $J^{PC}=3^{--}$ assignment.

All predicted levels have a simple isospin structure (one isomultiplet) which implies that $\sigma(\bar{p}p \to \bar{p}p)/\sigma(\bar{n}n \to \bar{n}n)=1$. The experimentally determined branching ratio of the $M(2020)$ into $\bar{p}p$ is $>14\%$, so the branching ratio into $N\bar{N}>28\%$, which rules out color-sextet states. Since no charged partners of the $M^0(2020)$ have been found, the $I=0$, $J^{PC}=3^{--}$ assignment is preferred. Also, the absence of $M(2020)\pi$ final states in the decay of $M(2204)$ can be interpreted in favor of an $I=0$ assignment.

The discovery of $M^{\pm}(2020)$ states would be evidence for an $I=1$ state. Considering the accessible two-meson final states ($\pi\pi$, $K\bar{K}$, $\pi\rho$, $\rho\rho$), one expects the $J^{PC}=3^{++}$ to be most stable.

Color-triplet levels which can be assigned to the $M^0(2204)$ state are the $n_s=0$ $l^P=2^+$ levels at 2.23 and 2.24 GeV which have a complex isospin structure. We prefer the $J^{PC}=3^{++}$ assignment. The $J=1$ and 2 states couple to the $N\bar{N}$ $P$ waves and are expected to be more unstable than the $J=3$ and 4 ones, which couple to the $N\bar{N}$ $F$ waves. Absence of $K\bar{K}$ and $\pi\pi$ final states eliminates $J^{PC}=4^{++}$. This level has both $I=0$ and $I=1$ members. Until now no $M^{\pm}(2204)$ states have been reported from the same source. However, at 2.207 GeV an isovector state has been found in $\pi^-p \to \pi_F^+(K^+K^-\pi^-)$. It is not clear whether this state belongs to the same multiplet as the $M(2204)$. It may as well be a candidate for the $n_s=2$ $l^P=1^-$ color-triplet level predicted at 2.21 GeV, since no corresponding signal in $3\pi$ has been reported.

These assignments for the $M(2204)$ and $M(2020)$ are consistent with the (experimental) absence of the decay $M(2204) \to M(2020)\pi$.

The narrow $N\bar{N}$ resonances below 2 GeV are all predicted to have negative parity. Positive-parity states detected in this region should be attributed to the $n_s=0$ $l=3$ $Q\bar{Q}$ resonances (Table IV), e.g., the broad resonance with $J^P=2^+$ or $4^+$ seen in $\bar{p}p \to \rho^0\omega^0 \to 5\pi$ at 1.95 GeV.[22] It has a strong coupling to mesonic decay modes and a small to middle-sized elasticity: $x=0.135^{+0.13}_{-0.06}$.

Interesting phenomena involving baryonium states may also be present below the $N\bar{N}$ threshold. Including the color-sextet baryonium states, we find in our calculation of the $Q^2\bar{Q}^2$ mass spectrum one $l^P=2^+$ and five $l^P=1^-$ levels below the $N\bar{N}$ threshold. The dominant decay mode of these states presumably is the multimeson one (Fig. 2). The levels at 1.76 and 1.83 GeV are probably more stable than the other ones. The first one has angular momentum $l=2$ and the latter contains an $s\bar{s}$ pair.

All $l^P=1^-$ levels contain a photonlike member, $J^{PC}=1^{--}$, $I=0$ or 1 (see Fig. 3), which suggests that their existence can be checked in $e^+e^-$ annihilation. Although the coupling of the diquark-antidiquark pair to the photon probably will not be as strong as that of the quark-antiquark pair, they may be detectable at, e.g., DCI.[16] Apart from many broad $e^+e^-$ resonances, several narrow ones have been reported (Table XX). More experimental data and calculations on the multimeson branching ratios are needed to distinguish the $Q^2\bar{Q}^2$ states from the orbitally and radially excited $Q\bar{Q}$ mesons in this region. The presence of photonlike $l=0$ $Q^3\bar{Q}^3$ states in this region presumably does not cause much trouble, since their coupling to $e^+e^-$ is expected to be still weaker than that of the baryonium states.

Important information on the baryonium states below threshold may be obtained from the $\gamma$-ray spectrum of atomic $\bar{p}p$ systems. Baryonium final states are found when the emitted photon results from the annihilation of a $Q\bar{Q}$ pair. Now all $J^{PC}$ members of the level at 1.72 GeV and at 1.76 GeV ($l=2$) can be reached. Decay to the highly degenerate level at 1.72 GeV may be quite attractive and one of the two higher $\gamma$-ray states (Table XX) may be assigned to it. In that case our mass values are about 100 MeV off. The $\gamma$ ray may also result from the coalescence of two three-quark bags into a single $l=0$ $Q^3\bar{Q}^3$ bag. Because these states usually simply fall apart to a three-meson final state, some of the high-spin or low-mass states may have a sufficiently restrictive final-state phase space to be narrow. These levels and complementary ones, like deeply bound $N\bar{N}$

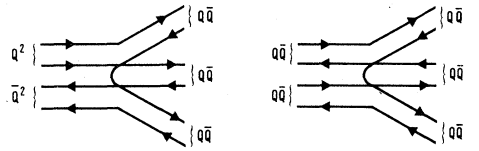


FIG. 2. Three-meson decay mode of baryonium (a) and 8-mesonium (b) states.

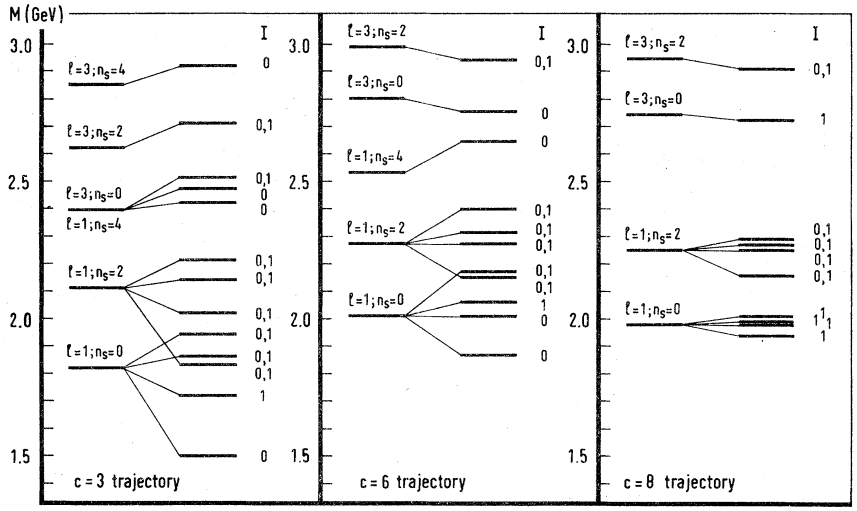


FIG. 3. Leading-trajectory states with photonlike quantum numbers: $J^{PC}=1^{--}$ and $Y=0$, as a function of the orbital angular momentum $l$ and the number of strange quarks $n_s$.

states, also might contribute to the experimental spectrum.

We note that the spectrum of narrow $e^+e^-$ resonances does not coincide with the atomic $\gamma$-ray spectrum. If we take the $\gamma$-ray states as serious candidates, this might indicate that none of the $e^+e^-$ resonances found until now (as a result of weak coupling) are baryonium ones or vice versa.

The most unambiguous candidate for $Q^2\bar{Q}^2$ states is the narrow, doubly charged strange resonance found in the reaction $K^+p \to (\bar{\Lambda}p\pi^+)n$ at 2.461 GeV. Though not quite significant it shows up as a peak in both the $\bar{\Lambda}\Delta^{++}(1232)$ and $p\bar{\Sigma}^+(1385)$ invariant mass plots. The production of such an exotic final state $(uu\bar{d}\bar{s})$ also requires the exchange of an exotic meson $(uu\bar{u}\bar{d})$.[6] In our model this state might be ascribed to the $l=3$ color-triplet baryonium $n=18$ level at 2.42 GeV. Another narrow strange state, seen in $\Lambda\bar{p}$ at 2.11 GeV, might be ascribed to the $l=2$ color-triplet baryonium $n=18$ level.[23]

This treatment of the orbitally excited $Q^2\bar{Q}^2$ system is by no means exhaustive. We only discussed the nature of a few prominent states and did not touch upon the status of the remaining ones. At present a detailed assignment of all reported states is not yet a feasible undertaking. The experimental status of many reported states is not completely resolved. Information about quantum numbers is still very scarce. Also, on the theoretical side sufficient knowledge of e.g. decay mechanisms is lacking.

Our mass formula is able to reproduce the $Q\bar{Q}$ and $Q^3$ (Ref. 1) mass spectrum quite well. Judging by the nice assignments for the lowest scalar-meson nonet and for prominent states like the $S(1936)$ we trust that it will work as well for the $Q^2\bar{Q}^2$ and other multiquark states. We hope it provides a useful reference frame in which one can, at least qualitatively, discuss results on experimental spectroscopy.

*Note added in proof.* In a recent analysis of the ACCMOR collaboration[41] the resonance parameters of the $A_1$ meson have been determined to be $M=1.28$ GeV and $\Gamma\simeq 0.3$ GeV. This mass is in agreement with the other $l=1$ $Q$-$\bar{Q}$ mesons. Reference 42 mentions a $J^P=6^+$ meson in a partial-wave analysis of the $p\bar{p}$ system in the reaction $\pi^-p \to p\bar{p}n$ with a mass of 2.71 GeV, in agreement with the predictions in Table XIII.

ACKNOWLEDGMENTS

We would like to thank Professor R. A. Bryan for reading the manuscript. Part of this work was included in the research program of the Stichting voor Fundamenteel Onderzoek der Materie (FOM) with financial support from the Nederlandse Organisatie voor Zuiver-Wetenschappelijk Onderzoek (ZWO).

*Present address: Los Alamos Scientific Laboratory, University of California, Los Alamos, N.M. 87545.

[1]P. J. Mulders, A. T. Aerts, and J. J. de Swart, Phys. Rev. D 19, 2635 (1979).
[2]A. Chodos, R. L. Jaffe, K. Johnson, and J. Kiskis, Phys. Rev. D 12, 2060 (1975).
[3]K. Johnson and C. B. Thorn, Phys. Rev. D 13, 1934 (1976); K. Johnson and C. Nohl, *ibid.* 19, 291 (1979) includes flavor breaking.
[4]A. T. Aerts, Nijmegen University thesis, 1979 (unpub-

lished).
[5]R. L. Jaffe, Phys. Rev. D 15, 267, 281 (1977).
[6]R. L. Jaffe and F. E. Low, Phys. Rev. D 19, 2105 (1979).
[7]R. L. Jaffe, Phys. Rev. D 17, 1444 (1978).
[8]Chan H.-M. and H. Högaasen, Phys. Lett. 72B, 121 (1977); Nucl. Phys. B136, 401 (1978).
[9]Chan H.-M. *et al.*, Phys. Lett. 76B, 634 (1978).
[10]J. C. Kluyver, Z. Phys. C 1, 3 (1979).
[11]For example, M. I. Machi, S. Otsuki, and F. Toyoda, Prog. Theor. Phys. 57, 517 (1977); X. Artur, Nucl. Phys. B85, 442 (1975); G. C. Rossi and G. Veneziano, Nucl. Phys. B123, 507 (1977).
[12]G. F. Chew and C. Rosenzweig, Phys. Rep. 41C (1978).
[13]See, e.g., I. S. Shapiro, Phys. Rep. 35C, 129 (1978).
[14]Particle Data Group, Phys. Lett. 75B, 1 (1978); see also S. O. Protopopescu and N. P. Samios, Brookhaven Report No. BNL-26077, 1979 (unpublished).
[15]S. Ozaki, Brookhaven Report No. BNL-25057 (unpublished).
[16]D. M. Tow, B. Nicolescu, and J. M. Richard, Nucl. Phys. B150, 287 (1979).
[17]L. Micu, Nucl. Phys. B10, 521 (1969).
[18]See, e.g., J. L. Rosner, Phys. Rep. 11C, 191 (1974).
[19]Chan H.-M. and Tsou S. T., Phys. Rev. D 4, 156 (1971); C. Quigg and F. von Hippel, *ibid.* 5, 624 (1972).
[20]R. L. Kelly and R. J. N. Phillips, Report Nos. RL-76-052 and LBL-4879 (unpublished).
[21]C. B. Dover and S. Kahana, Phys. Lett. 62B, 293 (1976).
[22]C. Defoix *et al.*, Collège de France, Report No. LPC/79-13; P. Espigat *et al*, Collège de France, Report No. LPC/79-14.
[23]C. Evangelista *et al.*, paper No. 521 contributed to the XIX International Conference on High Energy Physics, Tokyo, 1978 (unpublished).
[24]C. Defoix *et al.*, in *Proceedings of the 3rd European Symposium on Antinucleon-Nucleon Interactions, Stockholm*, edited by G. Ekspong and S. Nilsson (Pergamon, Oxford and New York, 1976), pp. 169 and 175.
[25]A. A. Carter *et al.*, Phys. Lett. 69B, 117, 122 (1977); Nucl. Phys. B141, 467 (1978); in *Proceedings of the 3rd European Symposium on Antinucleon-Nucleon Interactions, Stockholm* (Ref. 24), p. 139.
[26]R. J. Abrams *et al.*, Phys. Rev. D 1, 1917 (1970); J. Alspector *et al.*, Phys. Rev. Lett. 30, 1511 (1973); M. Coupland *et al.*, Phys. Lett. 71B, 460 (1977).
[27]P. Pavlopoulos *et al.*, Phys. Lett. 72B, 415 (1978).
[28]C. Bemporad, work presented at Hamburg International Conference on Lepton and Photon Interactions, 1977 (unpublished).
[29]L. Gray *et al.*, Phys. Rev. Lett. 26, 149 (1971).
[30]L Gray *et al.*, Phys. Rev. Lett. 30, 1091 (1973).
[31]T. E. Kalogeropoulos and G. S. Tzanakos, in *Proceedings of the 3rd European Symposium on Antinucleon-Nucleon Interactions, Stockholm* (Ref. 24), p. 29.
[32]A. S. Carroll *et al.*, Phys. Rev. Lett. 32, 247 (1974); V. Chaloupka *et al.*, Phys. Lett. 61B, 487 (1976); O. Braun *et al.*, Nucl. Phys. B124, 45 (1977).
[33]D. Cutts *et al.*, Phys. Rev. D 17, 16 (1978); S. Sahamoto *et al.*, paper No. 1058 contributed to the XIX International Conference on High Energy Physics, Tokyo, 1978 (unpublished).
[34]M. Wong *et al.*, paper No. 220 contributed to the XIX International Conference on High Energy Physics, Tokyo, 1978 (unpublished).
[35]D. E. Caro *et al.*, in *Proceedings of the 4th International Conference on Antinucleon-Nucleon Interactions, Syracuse, New York, 1975*, edited by T. E. Kalogeropoulos and K. C. Wali (Syracuse University, Syracuse, 1975), Vol. III, p. 13; A. Subramanian, in *Proceedings of the 3rd European Conference on Antinucleon-Nucleon Interactions, Stockholm* (Ref. 24), p. 51.
[36]P. Benkheiri *et al.*, Phys. Lett. 68B, 483 (1977); 81B, 380 (1979); B. G. Gibbard *et al.*, Phys. Rev. Lett. 42, 1593 (1979).
[37]M. Baubillier, in Proceedings of the Workshop on Baryonium and Other Unusual States, Orsay, France, 1979 (unpublished).
[38]D. R. Green *et al.*, paper No. 810 contributed to the XIX International Conference on High Energy Physics, Tokyo, 1978 (unpublished).
[39]T. A. Armstrong *et al.*, paper No. 608 contributed to the XIX International Conference on High Energy Physics, Tokyo, 1978 (unpublished).
[40]H. Braun *et al.*, Phys. Lett. 60B, 481 (1976).
[41]C. Daum *et al.*, CERN Report No. CERN-EP/79-110, 1979 (unpublished).
[42]M. Rozanska *et al.*, CERN Report No. CERN-EP/79-86, 1979 (unpublished).